

# **Experimental Investigation of the Effect of Absorber Plate Temperature on Double Slope Inclined Solar Water Desalination Still**

**Maziar Salimizad**

Submitted to the  
Institute of Graduate Studies and Research  
in partial fulfilment of the requirements for the Degree of

Master of Science  
in  
Mechanical Engineering

Eastern Mediterranean University  
September 2014  
Gasimağusa, North Cyprus

Approval of the Institute of Graduate Studies and Research

---

Prof. Dr. Elvan Yılmaz  
Director

I certify that this thesis satisfies the requirements as a thesis for the degree of Master of Science in Mechanical Engineering.

---

Prof. Dr. Uğur Atikol  
Chair, Department of Mechanical Engineering

We certify that we have read this thesis and that in our opinion it is fully adequate in scope and quality as a thesis for the degree of Master of Science in Mechanical Engineering.

---

Assoc. Prof. Dr. Mustafa İlkan  
Co-Supervisor

---

Prof. Dr. Fuat Egelioglu  
Supervisor

---

Examining Committee

1. Prof. Dr. Uğur Atikol

2. Prof. Dr. Fuat Egelioglu

3. Assoc. Prof. Dr. Hasan Hacısevki

---

---

---

## ABSTRACT

Solar energy can be used for potable water production from brackish water. In this study the effect of the absorber plate temperature on the inclined solar water desalination having double sloped cover (DS-ISWD) performance was experimentally studied. The DS-ISWD system with net cavity area of  $1.5 \text{ m}^2$  was constructed and it has two slope glazing; each inclined  $25^\circ$  and four spray jet nozzles were installed at equal intervals within the DS-ISWD. The experience gained from the operation of spray jet solar desalination at the Eastern Mediterranean University, N. Cyprus has revealed the importance of feeding water volume on the system performance. The DS-ISWD system with four jet sprays was tested with different on set temperatures of 40, 45, 50, 55,  $60^\circ\text{C}$  in spring (April). The maximum daily yield achieved was  $3.85 \text{ kg/day m}^2$  when the absorber plate temperature was kept at  $55^\circ\text{C}$ . The fresh water yield at 40, 45, 50, 55, and  $60^\circ\text{C}$  absorber plate temperatures were 3.6, 3.71, 3.72, 3.85 and  $3.68 \text{ kg/day m}^2$  respectively. It was observed that when the onset temperature was set  $65^\circ\text{C}$  the pump was not in operation after 14:00 hrs. This indicates that the absorber plate temperature was less than  $65^\circ\text{C}$  so the system stops generating fresh water after 14:00 hrs. Therefore, the  $65^\circ\text{C}$  plate temperature was ignored in spring tests. The daily average efficiency of DS-ISWD system was observed to be 33.8% for  $55^\circ\text{C}$  set-point temperature. The effect of continuous water spraying on the DS-ISWD productivity was also examined. When the absorber plate was at  $40^\circ\text{C}$  the pump operated continuously i.e., the feedwater was continuous.

The experiments were also conducted in July and the optimum absorber temperature was found to be  $65^\circ\text{C}$  with  $4.2 \text{ kg/day m}^2$  of fresh water production. At  $60^\circ\text{C}$  the

pump operated continuously and the fresh water production was 5% less than the optimum whereas, the production was decreased by 5% when the absorber plate was at 70°C.

From the obtained results it can be concluded that the performance of the DS-ISWD depends on the absorber plate temperature. The DS-ISWD performance also depends on the solar insolation, feedwater temperature, sprayed water size and other climatic parameters.

**Keywords:** Potable water, inclined solar water desalination, absorber plate temperature, thermal efficiency

## ÖZ

Güneş enerjisi tuzlu sudan içme suyu üretimi için kullanılabilir. Bu çalışmada, absorber levha sıcaklığının, eğimli güneş su arıtma (EGSA) sisteminin performansına etkisi deneysel olarak incelenmiştir. Net alanı  $1.5 \text{ m}^2$  olan  $25^\circ$  eğimli iki cam örtülü EGSA sistemi yapılmıştır; dört püskürtme nozulu EGSA içerisine eşit aralıklarla monte edildi. Doğu Akdeniz Üniversitesi'nde püskürtme başlıkları kullanılarak güneş su arıtmasında kazınan deneyimlerden giriş suyu hacminin EGSA sistem performansına olan önemi ortaya konulmuştur. Dört püskürtme nozulu EGSA sistemi ilkbaharda (Nisan) absorber plakası ayarlanan farklı sıcaklıklarda  $40, 45, 50, 55, 60^\circ\text{C}$  pompa çalıştırılarak test edildi. Maksimum günlük verim plaka sıcaklığı  $55^\circ\text{C}$  olduğu günde  $3.85 \text{ kg/gün m}^2$  olarak elde edildi. Absorber plaka sıcaklıkları  $40, 45, 50, 55, 60^\circ\text{C}$  ye ayarlandığı zaman arıtılmış su üretimi sırasıyla  $3.6, 3.71, 3.72, 3.85$  ve  $3.68 \text{ kg/gün m}^2$  idi. Absorber sıcaklığı  $65^\circ\text{C}$  ayarlandığında pompanın saat 14:00 ten sonra çalışmadığı ve su arıtması olmadığı gözlemlendi, bunun nedeni absorber levha sıcaklığının saat ikiden sonra  $65^\circ\text{C}$  az olmasıdır. Bu nedenle,  $65^\circ\text{C}$  levha sıcaklığı ilkbahardaki testlerde göz ardı edildi. EGSA sistemin  $55^\circ\text{C}$  levha sıcaklığındaki ortalama günlük verimliliği %33.8 olduğu görülmüştür. Sürekli su püskürtmenin EGSA üretimine etkisi incelendi. Absorber levha sıcaklığı  $40^\circ\text{C}$  ayarlandığı zaman pompanın sürekli çalıştığı gözlemlendi, yani giriş suyu sürekli dir.

Deneyler Temmuz ayında da yapıldı ve optimum levha sıcaklığı  $65^\circ\text{C}$  olup elde edilen günlük tatlı su  $4.2 \text{ kg/gün m}^2$  dir.  $60^\circ\text{C}$  levha sıcaklık ayarında pompa sürekli

alıřtı ve retim optimum retimden %5 daha azdı, absorber levha sıcaklıęı 70°C ayarlandığında retim optimumuna gre %5 azaldı.

Elde edilen sonulara gre, EGSA nın performansı absorber levha sıcaklıęına, baęlı olduęu sonucuna varılabilir. EGSA nın performansı aynı zamanda gneř radyasyonuna, giriř suyunun sıcaklıęına, pskrtlen su damlalarının byklęne ve dięer iklim a parametrelerine de baęlıdır.

**AnahtarKalimeler:** İilebilir su, eęimli gneř su arıtma, absorber levha sıcaklıęı, ısıl verimlilik.

## **ACKNOWLEDGMENT**

I would like to express my sincerely appreciation to my supervisor Prof. Fuat Eglioglu for his advice and interminable contribution to preparing this dissertation. Without his invaluable support accomplishment of this goal would not be possible for me.

To my parents, I would like to thank you for supporting me and putting up with me in difficulties, specially their encouragement to pursue my career goals.

# TABLE OF CONTENTS

ABSTRACT.....	iii
ÖZ.....	v
ACKNOWLEDGMENT.....	vii
LIST OF TABLES.....	x
LIST OF FIGURES.....	xi
LIST OF SYMBOLS.....	xiii
1 INTRODUCTION.....	1
1.1 Overview.....	1
1.2 Desalination.....	2
1.3 Desalination Methods.....	2
1.4 Thesis Objective and Organization.....	4
2 LITERATURE REVIEW.....	7
2.1 Solar Desalination Systems.....	7
2.2 Direct Solar Water Desalination System.....	8
3 THEORETICAL APPROACH AND EXPERIMENTAL PROCEDURE.....	13
3.1 Introduction.....	13
3.2 Mathematical Modeling of the System.....	14
3.3 The DS-ISWD System.....	16
3.3.1 Pump.....	19
3.3.2 Spray Nozzles.....	19
3.3.3 Glass Cover.....	21
3.3.4 Cavity.....	21
3.3.5 The Absorber Plate.....	22



3.4 Experimental Set-Up and Instrumentation.....	22
3.4.1 System Operation.....	22
3.4.2 Thermocouples.....	24
3.4.3 An Eppley Pyranometer.....	24
3.4.4 Temperature Controller.....	26
4 RESULTS AND DISCUSSION.....	27
4.1 Spring Results.....	27
4.2 Parameters Affecting the Performance of the DS-ISWD.....	39
4.3 Summer Results.....	41
4.4 Economical Analysis.....	48
5 CONCLUSION AND RECOMMENDATIONS.....	51
REFERENCES.....	53

## LIST OF TABLES

Table 3.1. Water pump details .....	19
Table 4.1. Components price .....	49

## LIST OF FIGURES

Figure 1.1. Thermal and membrane desalination process.....	3
Figure 2.1 Parameters affecting basin type solar still productivity [23] .....	12
Figure 3.1. Schematic of the DS-ISWD.....	15
Figure 3.2. The front sectional view of the DS-ISWD .....	17
Figure 3.3. The pictorial schematic diagram of the DS-ISWD.....	17
Figure 3.4. Left: top pictorial view, Right: side view of the DS-ISWD .....	18
Figure 3.5. Shows Water Motor Pump (Model QB-60) .....	19
Figure 3.6. Spray jets arrangement .....	20
Figure 3.7. Diagram of spray jets distances.....	21
Figure3.8. System operating diagram .....	23
Figure 3.9. Two-channel digital thermometer (DM6802A series digital, VICHY) .	25
Figure 3.10. An Eppley Pyranometer.....	25
Figure 3.11. Temperature controller (nux hanyoung, model:BR6) .....	26
Figure 4.1. Solar radiation at 40 °C set point temperature .....	29
Figure 4.2. Pure water outcome at 40 °C set temperature.....	29
Figure 4.3. Glass temperature and ambient air condition in 40 °C set temperature...	30
Figure 4.4. Solar radiation at 45 °C set point temperature.....	30
Figure 4.5. Pure water outcome at 45 °C set temperature.....	31
Figure 4.6. Glass temperature and ambient air condition in 45 °C .....	31
Figure 4.7. Solar radiation at 50 °C set point temperature.....	32
Figure 4.8. Pure water outcome at 50 °C set temperature.....	32
Figure 4.9. Glass temperature and ambient air condition in 50 °C set temperature...	33
Figure 4.10. Solar radiation at 55 °C set point temperature.....	33

Figure 4.11. Pure water outcome at 55 °C set temperature.....	34
Figure 4.12. Glass temperature and ambient air condition in 55 °C .....	34
Figure 4.13. Solar radiation at 60 °C set point temperature.....	35
Figure 4.14. Pure water outcome at 60 °C set temperature.....	35
Figure 4.15. Glass temperature and ambient air condition in 60 °C .....	36
Figure 4.16. Daily average pure water at various set temperature in spring.....	36
Figure 4.17. Hourly efficiencies of the DS-ISWD in spring .....	40
Figure 4.18. Daily average efficiency at various set temperatures in spring .....	40
Figure 4.19. Daily average efficiency at various set temperatures in spring including pump work.....	41
Figure 4.20. Solar radiation at 60 °C set point temperature.....	42
Figure 4.21. Pure water outcome at 60 °C set temperature.....	42
Figure 4.22. Glass temperature and ambient air condition in 60 °C .....	43
Figure 4.23. Solar radiation at 65 °C set point temperature.....	43
Figure 4.24. Pure water outcome at 65 °C set temperature.....	44
Figure 4.25. Glass temperature and ambient air condition in 65 °C .....	44
Figure 4.26. Solar radiation at 70 °C set point temperature.....	45
Figure 4.27. Pure water outcome at 70 °C set temperature.....	45
Figure 4.28. Glass temperature and ambient air condition in 70 °C .....	46
Figure 4.29. Daily average pure water at various set temperature in summer.....	46
Figure 4.30. Hourly efficiencies of the DS-ISWD in summer .....	47
Figure 4.31. Daily average efficiency at various set temperatures in summer .....	48
Figure 4.32. Daily average efficiency at various set temperatures in summer including pump work.....	49
Figure 4.33. Saving and cost Vs. water produced.....	50

## LIST OF SYMBOLS

$M$	Mass ( $\text{kg/m}^2$ )
$C$	Specific heat ( $\text{J/kg K}$ )
$T$	Temperature ( $^{\circ}\text{C}$ )
$h$	Convection heat transfer coefficient ( $\text{W/m}^2\text{C}$ )
$h_{fg}$	Latent heat of vaporization ( $\text{J/kg}$ )
$T$	Temperature of the atmosphere ( $^{\circ}\text{C}$ )
$\dot{m}$	Mass flow rate ( $\text{kg/s}$ )
$L$	Length
$W$	Width
$H$	Latent heat of vaporization ( $\text{J/kg}$ )
$I$	Solar radiation ( $\text{W/m}^2$ )
$A$	Area ( $\text{m}^2$ )
$Q$	heat transfer ( $\text{W}$ )
$p$	Pump work input ( $\text{Wh}$ )

### *Greek symbols*

$\alpha$	Absorptivity of absorber plate
$\varepsilon$	Emissivity of absorber plate
$\tau$	Transmissivity of glass
$\rho$	Density( $\text{kg/m}^3$ )
$\eta$	Efficiency

## Subscripts

<i>ab</i>	absorber plate
<i>ev</i>	evaporation
<i>g</i>	Glass
<i>at</i>	atmosphere
<i>T</i>	total
<i>b</i>	<i>base</i>
<i>i</i>	<i>instantaneous</i>
<i>w</i>	<i>water</i>

# Chapter 1

## INTRODUCTION

### 1.1 Overview

The demand for fresh water has been increased with growing population. Moreover, domestic and industrial pollution of fresh water resources are adversely affecting the situation. Underground water reservoirs have been used for ages to supply the fresh water requirements of the inhabitants. Excessive water drawing from the underground freshwater resources increased the salinity and some of those resources become useless.

Water is an essential ingredient for the existence of life. Water is needed for life. When there is water shortage, serious problems may arise. At present, in many places water is not edible spontaneously unless it is treated. More than 70% of the earth crust is covered by water; these water bodies contain both the fresh and the salty water bodies. The salty water bodies are around 97.5% while 2.5% of the remaining is fresh water. 80% of fresh water is frozen in the icebergs or combined as soil moisture. The frozen soil icebergs and the trapped water are inaccessible for human use. Salty water is not good for direct human use while the fresh water bodies are available for human consumption can be used if not polluted domestically and/or by industrial wastes [1]. In North Cyprus, the water shortage has grossly affected farm land irrigation; annually 125,984,118 m<sup>3</sup> of fresh water is needed to meet the country demands, while the various aquifers can contribute 74 million m<sup>3</sup>. This resulted in a

decline in the yearly quantity of agricultural produce as vast quantities of arable land suffer from low yield due lack insufficient irrigation.

Water shortage, climate change and rising costs of fossil fuels are the major global concerns that will continue to affect the whole world in this century. New, sustainable and renewable energies can play the significant role in meeting the demand of these shortages. Solar desalination is one of the many processes used in purifying water for domestic and agricultural use. However, solar desalination generally has a low productivity. There are many studies which were conducted to increase the productivity of solar desalination systems such as utilizing external condensers, better insulation, cooling the glazing in solar stills, modifying the construction using inclined solar desalination systems and etc. Agboola and Egelioglu [2] experimentally investigated an improved incline solar water desalination system.

## **1.2 Desalination**

Desalination is the process of removing salts and minerals from seawater or brackish water. It is also called desalting. Desalination produces drinking water and concentrates were removed in the desalination process. Desalination process needs energy for separation of salt and dissolved materials from brackish to produce fresh water. Intensive and huge energy requirement is necessary in most desalination plants [3].

## **1.3 Desalination Methods**

Desalination procedures depend on energy used and can be classified into three main categories: thermal desalination, mechanical desalination (membrane desalination) and electrical desalination processes. In all three processes, either the evaporation is



followed by condensation forming pure water or freezing following melting of the formed water ice crystals. Figure 1.1 shows desalination processes. Evaporation process might occur due to heat transfer over an area. The multistage flash desalination (MSF), solar stills, humidification-dehumidification (HDH) and single effect vapor compression (SEE) involve evaporation process. Two points make solar stills and HDH differ from other evaporation processes; 1- Water evaporates at lower temperatures compared to its boiling temperature. 2- The principal driving force for evaporation is the difference in concentration of water in air.

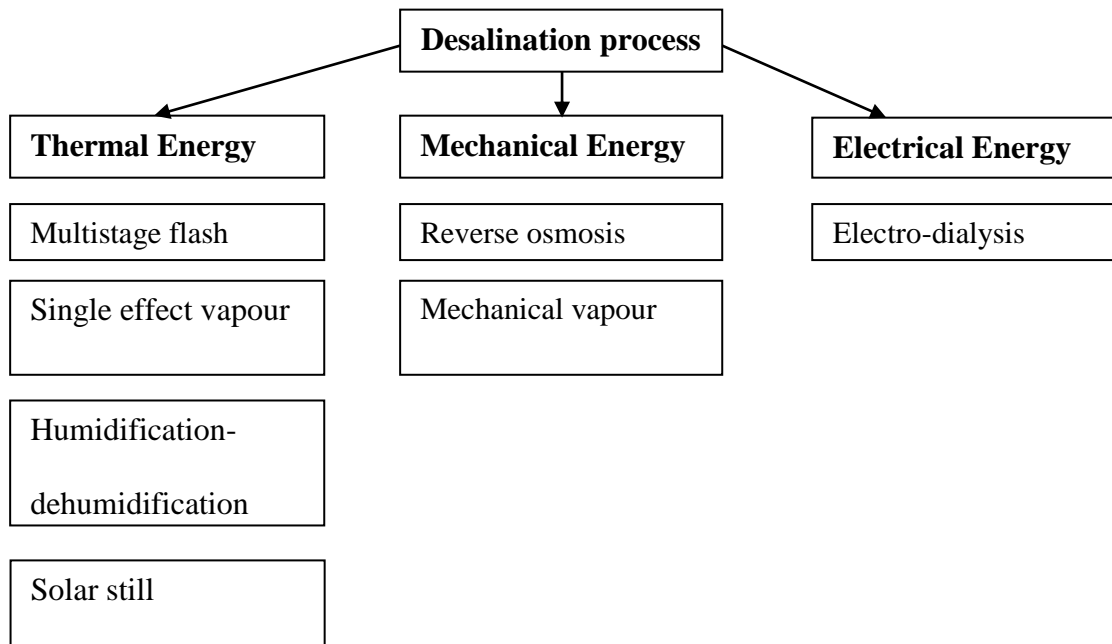


Figure 1.1. Thermal and membrane desalination process

Thermal desalination process remains the most widely used method of all the desalination systems. Desalination systems require a huge amount of energy and due to this, there is an increase interest in the use of renewable energy for desalination processes. Thermal energy process is classified into two classes where energy is either added or removed. Multistage flash and humidification-dehumidification

(HDH) are processes where energy is added. Freezing is a process where energy is removed from the brackish water.

Types of mechanical energy desalination include reverse osmosis (RO) and Mechanical Vapor compression (MVC). Mechanical energy in RO process forces water via the membrane while the salt remains in the brine stream. RO is the chief desalination process whereby fresh water diffuses via a semi-permeable membrane allowing a brine solution of high concentration. In an MVC process, the pressure and temperature difference of vapor compressor used to distillate water across the membrane as a latent heat for evaporation. Another membrane process is Electro dialysis (ED). This technique uses electrical energy as its driving force to move the electrically charged salt ions via a selective exchange membrane to produce a low salinity in one side of the membrane and high concentrated brine stream on the other side of the membrane [4].

#### **1.4 Thesis Objective and Organization**

It is well known that decreasing water depth is one of the key features to boost the performance of solar stills. El-Zahaby et al. [5] indicated that most recent studies tackling the water depth feature to improve the performance is limited. In their study in order to enhance the solar still performance they employed spray feeding to create a thin film of saline water in the solar still.

In the last few decades, many studies on factors that affect the efficiency and productivity of solar stills have been accomplished. Inclined solar water desalination as a promising technology previously investigated by Aybar et al [6] using a conventional incline solar water desalination (DS-ISWD), and Agboola and

Egelioglu [2] by utilizing spray jets in the DS-ISWD. In both studies, single sloped glazing systems were built and experimentally investigated in which water was continuously supplied as thin film onto the absorber plates. The absorber plate in each study was continuously cooled by the feedwater and the effect of the absorber plate temperatures on the yield were not investigated in their study.

In this study the main objective is to experimentally investigate the effect of the absorber plate temperature on fresh water yield in an ISWD system. A digital controller was installed to activate the pump for spraying feedwater as the absorber temperature reaches at the specified temperature. In the present system, a double slope glazing DS-ISWD system was constructed and 4 spray jets were intermittently operated in order to keep the absorber plate temperature at the required level. Finding an optimum temperature of the absorber plate can result in reducing power consumption and better design performance. Therefore, in order to achieve the main objectives the followings were done:

- a. An inclined solar water desalination system with double sloped glazing was constructed
- b. 4 spray jets were employed to spray water onto the absorber plate in order to enhance the heat transfer from the absorber plate to the sprayed water droplets.
- c. A thermo-switch was installed to the system in order to control the absorber plate temperature by activating and deactivating the pump which pumps salty feedwater onto the absorber plate via nozzles.

The chapters of thesis were arranged and organized as follows:

- The first chapter is the introduction; water shortage and desalination types are briefly discussed.
- The second chapter presents review of previous studies that is relevant to the study; links the topic of the thesis with the present literature.
- The third chapter presents the experimental procedure and instrumentations carried out to collect data and investigating the research work outcomes.
- The fourth chapter highlights the findings of this study and recommends future initiatives for developing this technology.
- Conclusions and recommendations are presented in chapter 5.

## **Chapter 2**

### **LITERATURE REVIEW**

#### **2.1 Solar Desalination Systems**

Solar desalination systems are systems which utilizes solar energy as the source of energy to separate water and salt. Solar desalination systems' classifications vary depending on its supply of energy or the technique employed. The most widely used type of solar system designs is solar stills. Solar stills can be classified into active and passive solar stills. It can also be classified based on its technique and design of its systems. This classification can also be based on whether the system is collection of direct or indirect. In the case of the direct collection system, all its sections are grouped into a single system using sustainable solar to evaporate salty water and condensate on the glass cover of the system such a system can be found in green house effects. The direct type of solar desalination system in the study of Garcia-Rodriguez, L et.al [7] was the main focus. The indirect collection system on the other hand makes use of two sub-systems. Energy collected from the Sun heats up and concentrates the salty water a sub-systems (via membrane) and the process of desalination occurs in the other sub-system. The DS-ISWD is a direct type solar desalination system, some of the direct type solar desalination systems available in the literature are presented in the following section.

## 2.2 Direct Solar Water Desalination Systems

According to the book of *Magiae Naturalis*, solar desalination discoveries date back to 1558. Up until now, there have been many researches done to improve productivity and efficiency on the solar desalination systems. The conventional solar stills which are widely known are direct desalination system. The solar still is generally made up of a basin, a single or double glass cover and an absorber plate. Several direct solar desalination systems have been produced from solar stills such as the inclined solar water desalination system. Aybar et al [6] in 2003 studied the effect of utilizing bare plate absorber, black fleece and black cloth on the productivity of the Inclined solar water desalination (ISWD) system. The results of their study indicated that the set up making use of the black fleece was the best configuration with daily production of  $2.995 \text{ kg/m}^2$ . Furthermore, they indicated that unequal distribution of feedwater results in unstable water evaporation. The rate of feeding flow is an important parameter. Evaporation increases when feeding water flow rate decreases, on the other hand the authors claimed that low rate of water supply can result in overheating the absorber plate which increases the rate of heat lost through the glass cover.

Inclined solar stills can be classified into traditional basin and wick solar stills. In a wick still, the feed water flows slowly through a porous material and thus evaporation rate is higher. An inclined solar still can take the advantage of a better angle to the sun. Tanaka et al [8, 9] reported 20-50% higher productivity when titled wick solar still was used. The influence of cavity geometry on single and double slope solar stills was experimentally investigated by E. Rubio et al [10]. In order to evaluate the distillate yield of solar stills, the testing conditions were controlled

within the range. The results indicated that distillate production is independent of the cavity geometry for small stills. T. Rajaseenivasan and K.K Murugavel [11] theoretically and experimentally investigated work performance and the effect of varying the water mass of a double slope single basin and double basin solar stills. Comparison of both stills indicated that double basin produced 85% higher pure water with the maximum up to 2.99 liters per day. S. Nijmeh et al [12] constructed a single-basin with equal angle double-sloped covers using various absorbing materials (such as dissolved salts, violet dye, and charcoal) to investigate the efficiency of the still. They found dissolved salts, violet dye, and charcoal (covering 50% basin area) can provide daily efficiency of up to 26%, 29% and 17.3% respectively, while water and water with reflector have efficiencies of 14.8% and 15.8%. K. Abdennacer and T. Rachid, [13] numerically studied the effect of inclination angle on the productivity. They found an optimum angle of  $10^\circ$  enhances the evaporation-condensation of the collector and ideal depth of the basin water is at its minimum value. Edeoja, et al [14] investigated the effect of angle of cover inclination on the yield of a single basin solar still. They tested five solar basins with different inclinations of 4, 7, 10, 13, and 15 degrees, under the same operating conditions. The results indicated that 15 degree inclination had the highest efficiency compared to other solar basins. P. I. Ayav and G. Atagunduz [15] experimentally and theoretically studied solar distillation in a single basin with 38 degree glass inclination and an aluminum reflector assembled to the still. They found up to 85% efficiency when reflector were used. A.K. Sethi and V.K. Dwivedi [16] investigated double-sloped active solar still under forced circulation mode. The recorded data indicated the daily productivity of solar still reduces with increasing in water depth in the basin. The thermal efficiency was ranged from 13.55 to 31.07% for winter and peaked in summer months. R.

Rajanarhini et al. [17] studied the effect of varying thickness of insulation to find an optimum thickness of a double sloped wick-type solar still. They observed a minimum thickness of 0.06 m can perform better and provides a better production and performance. S. Shanmugan et al. [18] experimentally investigated the performance of a single-sloped single-basin solar still with sensible heat storage materials such as white marble stones, pebbles, black stones, calcium stones, and iron scraps. Through their experiment, they found the calcium stones in the basin with dripping increases the evaporation during a day. Furthermore, they mentioned dripping of saline water increases the temperature difference between top cover and water in the basin because of low thermal capacity. Alaudeen A. [19] studied a single-slope solar still with 6 mm thickness glass basin and tested with different heat storage materials like sand, wax, ethylene glycol, and zinc nitrate. They reported productivities as  $2.64 \text{ kg/m}^2$  for corrugated sheets,  $2.53 \text{ kg/m}^2$  for ethylene glycol,  $2.29 \text{ kg/m}^2$  for sponge,  $2.08 \text{ kg/m}^2$  for wax,  $2 \text{ kg/m}^2$  for zinc nitrate, and  $1.79 \text{ kg/m}^2$  for sand, in which corrugated sheet can provide nearly 43% more pure water compared to the conventional solar still. Mahmoud. I.M and S. K. Mahkamov [20] in their study, used a heat pipe evacuated tube solar collector, and they achieved about 9 kg of fresh water per day with 68% efficiency. Rahul Dev and G.N. Tiwari [21] constructed and experimentally investigated combination system of evacuated tubular collector and solar still and named it evacuated tubular collector integrated solar still (EISS). Their results showed that EISS system can produce  $630 \text{ kg/m}^2$  per year while a single slope SS can produce almost half of it (about  $327 \text{ Kg/m}^2$ ). Sousi A. [22] experimentally studied the effect of air mass flow rate and the temperature difference of the brackish water on the performance of a HDH system. The main component of this system was consisted of solar air/water heater collector with



double glazing, humidifier (evaporator), dehumidifier (condenser), circulating pump, fan and a storage tank. The results indicated that the air mass flow rate has a direct effect on fresh water productivity while the temperature difference has no effect on the system. The factors that can affect the functioning of the direct solar system was studied by various researchers and proposed by Ali. F. Muftah et al [23] are presented in Figure 2.1.

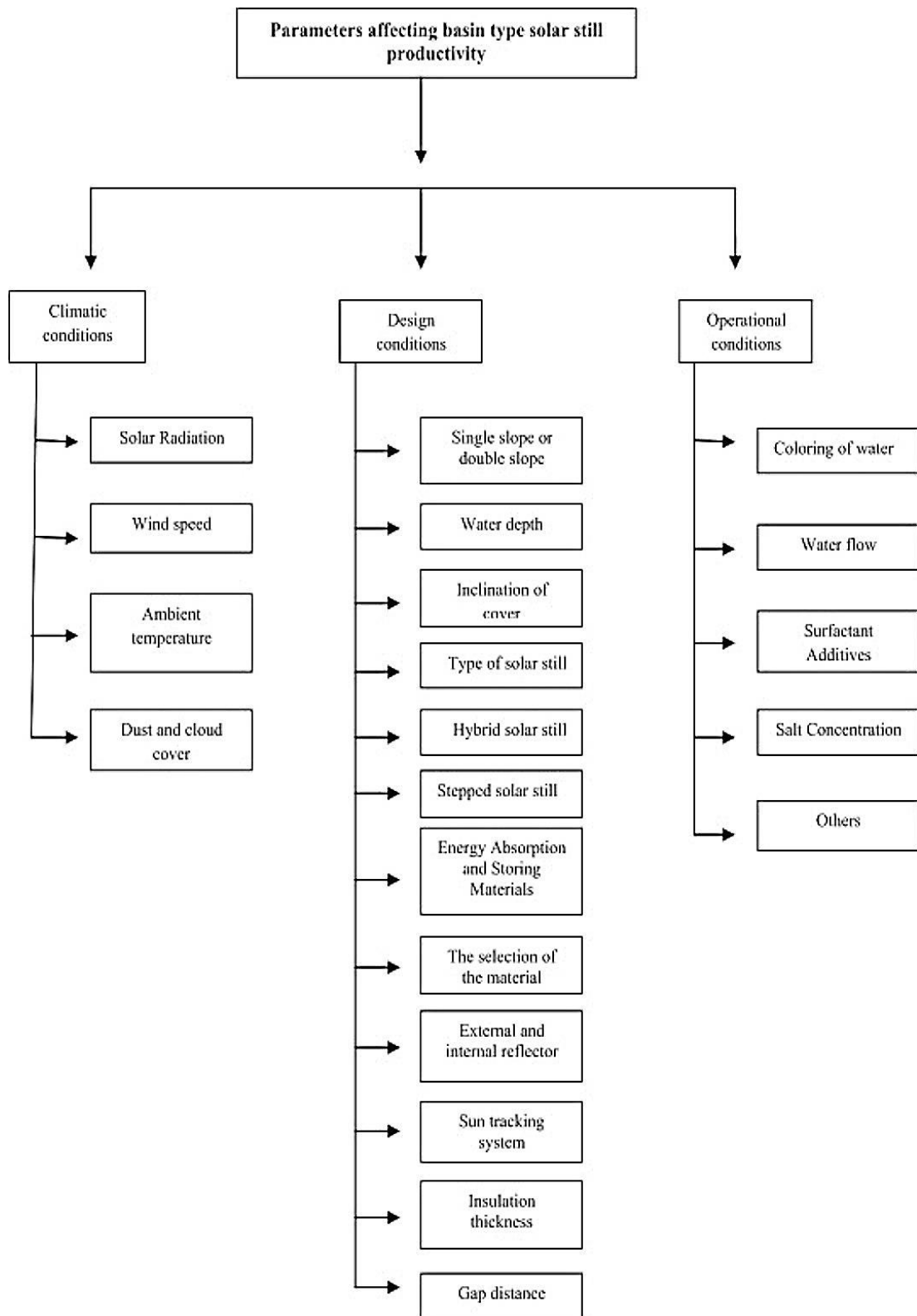


Figure 2.1. Parameters affecting basin type solar still productivity [23]

## Chapter 3

# THEORETICAL APPROACH AND EXPERIMENTAL PROCEDURE

### 3.1 Introduction

Spray cooling is employed where high heat transfer rate is required; such as electronic cooling applications. One of the advantages of spray cooling is the uniformity of heat removal. When droplets were hitting on the hot absorber plate of the DS-ISWD spread and evaporate or thin liquid film is formed. Large amount of heat transfer occurs as the droplets hit on the surface by evaporation, nucleate boiling, thin film convection and sometimes depending on the temperature of the absorber plate by transition boiling and etc. J. Kim [24] reviewed the spray cooling mechanism and indicated the areas where additional research is needed. The author indicated that the heat removal mechanisms during spray cooling are very complex. The main reason is the dependence of heat transfer on many parameters (such as droplet size distribution, velocity and droplet number density. The heat transfer is also affected by the orientation and surface roughness of the absorber plate and the number of spray jets. Xie et al. [25] derived a mathematical model to investigate thin film flow of spray impingement and they also developed a model to investigate the heat transfer performance in the non-boiling regime.

Zahaby et al [5] used transverse reciprocating spraying system to control the depth of water on a corrugated stepped shape absorber of solar still. They indicated that the

performance of the solar still was increased due to very low warming up period of thin film saline water. The authors indicated that the film thickness is not sensitive to nozzle inlet pressure but rather it is related to droplet flux.

As mentioned earlier Aybar et al [6] experimentally investigated a conventional DS-ISWD system. Agboola and Egelioglu [2] experimentally investigated an improved DS-ISWD where water was sprayed onto the absorber plate continuously. In the present study it is aimed to evaporate the sprayed water by transferring heat to water from the absorber plate (i.e., spray cooling of absorber plate) in order to improve the performance of the proposed DS-ISWD. As the spraying process was controlled by the temperature controller unit, the spraying period depends on the incoming solar radiation, absorber plate temperature, heat transfer rate from the plate to sprayed water and etc. As mentioned earlier the process is very complex and depends on several parameters. A simplified mathematical modeling of an DS-ISWD system is presented in the following section.

### 3.2 Mathematical Modeling of the System

A time dependent energy balance and mass balance equations for the DS-ISWD (Fig 3.1) are given below.

The energy equation of the absorber plate is

$$M_{ab}C_{ab} \frac{dT_{ab}}{dt} = I\tau\alpha - Q_{r,ab-g} - Q_{c,ab-w} \quad (3.1)$$

where  $M_{ab}$  is the mass of the absorber plate per unit area,  $C_{ab}$  is the specific heat of absorbing plate material,  $T_{ab}$  is the absorber plate temperature,  $I$  is the solar insolation,  $\tau$  is the transmissivity of glazing,  $\alpha$  is the absorptivity of the absorber plate.  $Q_{r,ab-g}$  is the radiation heat transfer from the absorber plate to the glass cover and  $Q_{c,ab-w}$  is the convection heat transfer from the absorber plate to water.

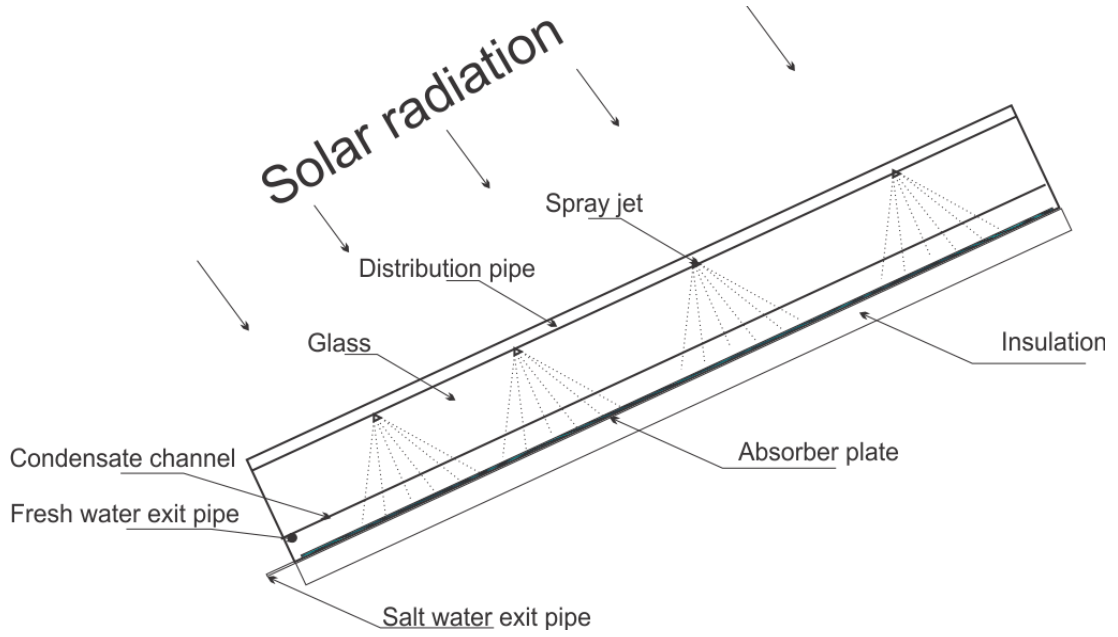


Figure 3.1. Schematic of the DS-ISWD

Equation 3.1 can be expressed in terms of heat fluxes as:

$$M_{ab}C_{ab} \frac{dT_{ab}}{dt} = I\tau\alpha - h_{r,ab-g}(T_{ab} - T_g) - h_{c,ab-w}(T_{ab} - T_w) \quad (3.2)$$

Where  $h_{r,ab-\mu}$  is the radiation heat transfer coefficient and  $h_{c,ab-w}$  is the convection heat transfer coefficient,  $T_g$  and  $T_w$  are the glass and water temperature respectively.

The radiation heat transfer coefficient equation is:

$$h_{r,ab-g} = \epsilon_{ab}\sigma(T_{ab} - T_g)(T_{ab}^2 + T_g^2) \quad (3.3)$$

Where,  $C_{ab}$  is the emissivity of absorber plate.

The energy equation of the glass cover is:

$$M_gC_g \frac{dT_g}{dt} = Q_{r,ab-g} + Q_{cond} - Q_{r,g-at} - h_{r,g-at}(T_g - T_{at}) - h_{c,g-at}(T_g - T_{at}) \quad (3.4)$$

Where  $Q_{r,ab-g}$ ,  $Q_{cond}$  and  $Q_{r,g-at}$  are the radiation heat transfer from the absorber plate to the glass, the condensation heat flux and the radiation heat transfer from the glass to atmosphere respectively.  $T_{at}$  is temperature of the atmosphere.

The energy equation of the water film on the absorber plate is:

$$\rho_w C_w y \frac{dT_{w,e}}{dt} = C_w (\dot{m}_i T_{w,i} - \dot{m}_e T_{w,e}) \frac{1}{L} + Q_{c,ab-w} - Q_{ev} \quad (3.5)$$

Where,  $\rho_w$  is the density of water,  $c_w$  is the specific heat of water,  $y$  is the water film thickness,  $L$  is the cavity length  $Q_{ev}$  is the evaporation heat transfer. The inlet water mass flow rate per unit width is  $\dot{m}_i$  and  $\dot{m}_e$  represents the exit mass flow rate per unit width. The difference between the inlet and exit mass flow rate is the fresh water obtained from the system.

The vapor mass balance equation is

$$\frac{dM_w}{dt} = (\dot{m}_{ev} - \dot{m}_{cond})LW \quad (3.6)$$

Where  $\dot{m}_{ev}$  and  $\dot{m}_{cond}$  are the evaporation and condensation mass flow rates.  $L$  is the length and  $W$  is the width of the cavity.

### 3.3 The DS-ISWD System

The main components of the set up are listed as follows:

- The cavity or bed,
- glass cover,
- pump
- spraying nozzles, and
- absorber plate.

Figure 3.2 shows the front sectional view of the DS-ISWD. The schematic diagram of the DS-ISWD is presented in Fig. 3.3 and Top view is presented in Fig. 3.4.

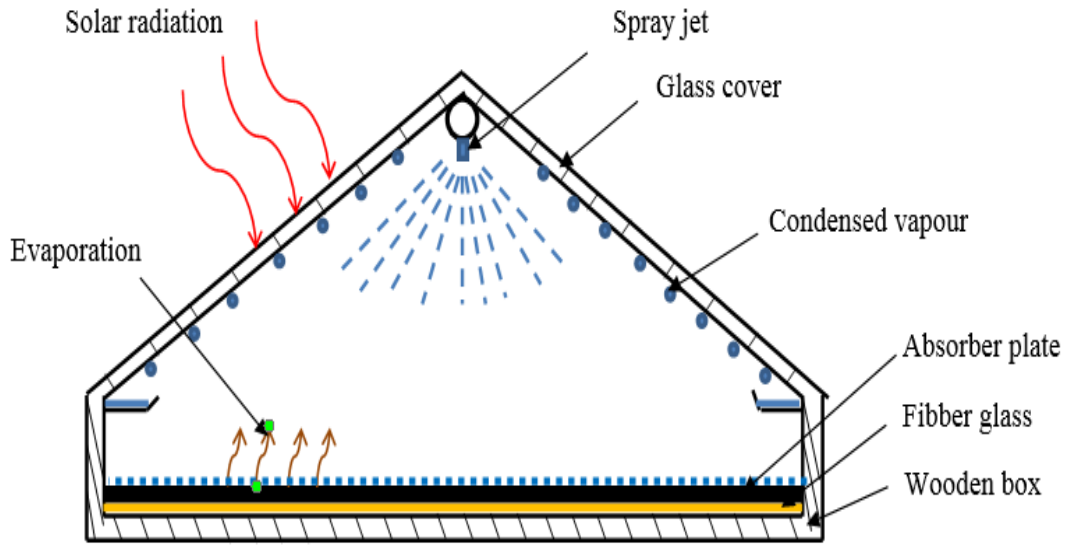


Figure 3.2. The front sectional view of the DS-ISWD

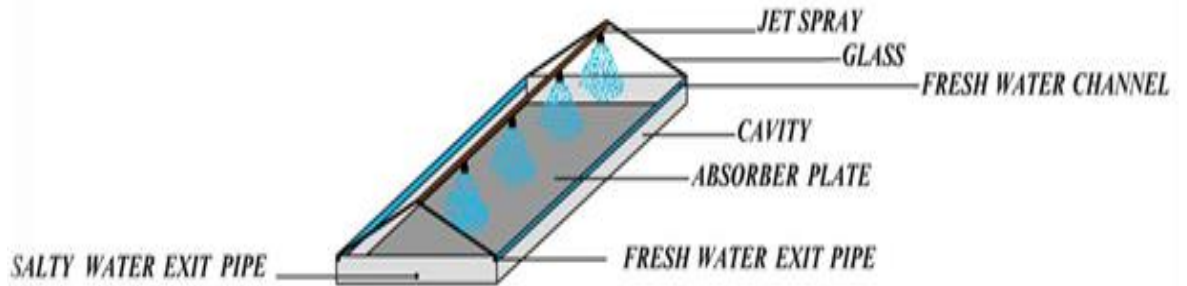


Figure 3.3. The pictorial schematic diagram of the DS-ISWD



Figure 3.4. Left: top pictorial view, Right: side view of the DS-ISWD



### 3.3.1 Pump

A single phase electro-mechanical pump was used to provide (45 liter/min) salty water to the DS-ISWD, the rating of motor was 0.45 HP (0.33 kW) The technical specification and picture of the pump can be found in Table 3.1 and Figure 3.5.

Table 3.1. Water pump details

Volume flow rate	Voltage	Hertz	Head max.	Suction max.	Power	RPM
35 L/min	240	50	35 m	9 m	0.45 HP	2850 m <sup>-1</sup>



Figure 3.5. Shows Water Motor Pump (Model QB-60)

### 3.3.2 Spray Nozzles

Water sprayed by nozzles evaporates quickly as water distributed in smaller quantities on the whole absorber plate. This technique provides a higher evaporation rate compared to continuous flow. In this study four nozzle were arranged in a line in the middle from top (See Figure 3.6) to the bottom above the absorber plate. Four jets sprays with 37cm distance between spray nozzles as shown in (figure-3.7) were used to spray the water when absorber plate temperature controller reaches the set point temperature.

In order to distribute feeding water, 7 mm diameter holes were equally spaced and drilled on feeding water pipe. These holes were used to connect the nozzle and to spray water at 70° hollow cone jet with 0.5-1 bar (50-100 kPa) pressure and 8-11 liters/min for each nozzle.

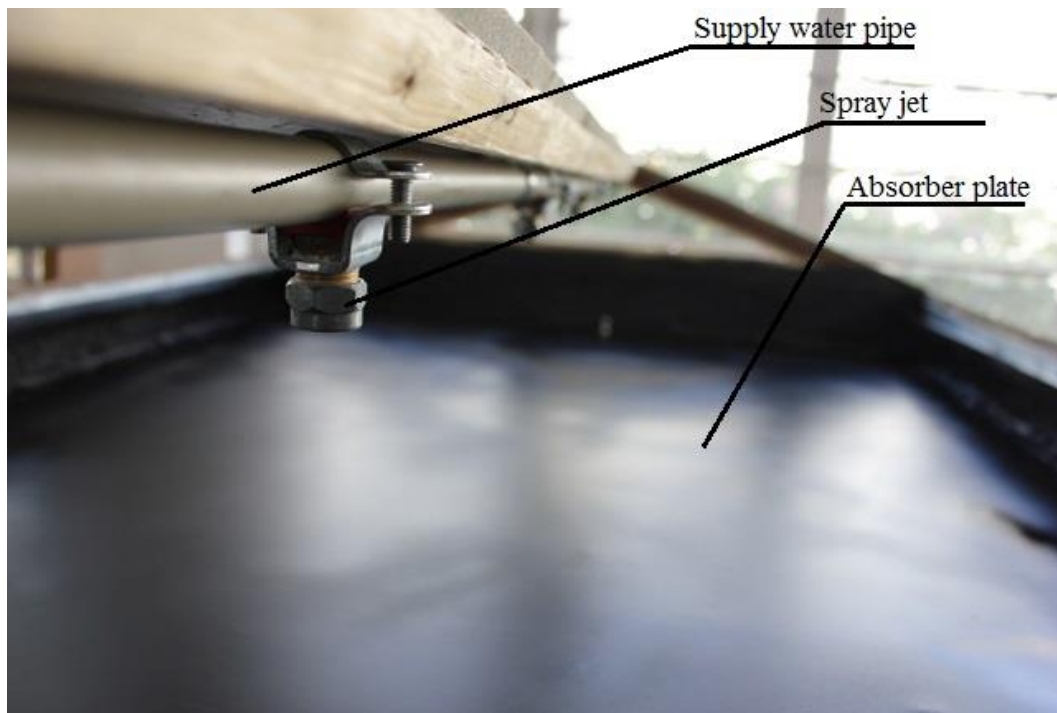


Figure 3.6. Spray jets arrangement

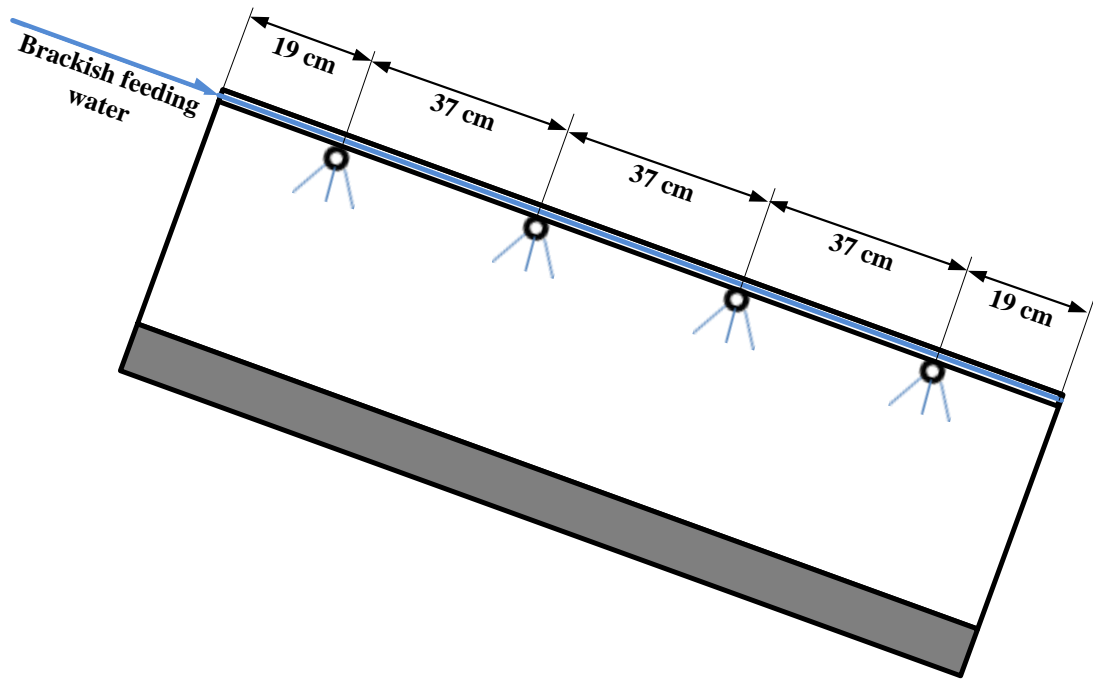


Figure 3.7 Diagram of spray jets distances

### 3.3.3 Glass Cover

The (DS-ISWD) glass covers consist of double slope glasses and a single triangular side glass. The top are each slum wide and 147 cm in length having 4 mm thickness and the side glass was located at the lower side of the box.

### 3.3.4 Cavity

The solar water desalination system holds its entire component in the form of box (cavity). The box which is used in solar water desalination setup is made of wood having 2 cm thickness. In order to avoid the possibility of water leakage from the box it is coated with 2.5 mm thick fiber glass.

The cavity which was designed for the DS-ISWD system is made of wood because it is fairly durable and has good insulation properties, the box is 1 m wide and 1.5 m long and its height is 0.2 m.

### **3.3.5 The Absorber Plate**

The insolation from the sun reaching to DS-ISWD is absorbed by the absorber plate which is constructed from galvanized steel painted in matte black. The absorber plate absorbs most of the solar radiation passing through the glass cover striking onto it. Absorber plate stores energy which depends on the thickness of the plate. The absorptivity of the absorber plate is increased by coating the surface with black paint. The hot absorber plate transfers heat to the sprayed water. The sprayed water partially evaporates as it absorbs energy when it comes in contact with the absorber plate. The absorber plate loses heat as cooler feedwater particles strikes onto it. Feedwater partly evaporates and the rest leaves the DS-ISWD with higher temperature. The vapor condenses on the glass cover and runs down to troughs at sides of the DS-ISWD and then collected within a container outside the DS-ISWD.

## **3.4 Experimental Set-Up and Instrumentation**

### **3.4.1 System Operation**

The constructed DS-ISWD was inclined 30° with horizontal in order to intercept more radiation. The sprayed water runs down the inclined absorber plate and drains from a hole that is located at the bottom lower end of box. As mentioned earlier in literature review, many studies have been conducted to investigate factors that are affecting the performance of solar desalination systems. The factors affecting the performance are the average temperature of the absorber plate, feeding water temperature, air cavity temperature, glass cover temperature and the amount of the feed water in the system. This study investigates the effect of absorber plate temperature on water desalination system. Therefore, the DS-ISWD system is designed to have intermittent spraying by using a temperature controller. The switch controller sensors were used to turn off the water supply when the absorber plate

temperature drops to a certain value and turns the pump on when the absorber plate temperature reaches to a specified value.

Brackish water which was not evaporated is heated as it comes into contact with the absorber plate drained out of system through a pipe located at bottom of the inclined box of the system and is collected in the storage containing the brackish water. Where evaporated water then condenses and collected as potable water. Figure 3.8 shows the system operating diagram.

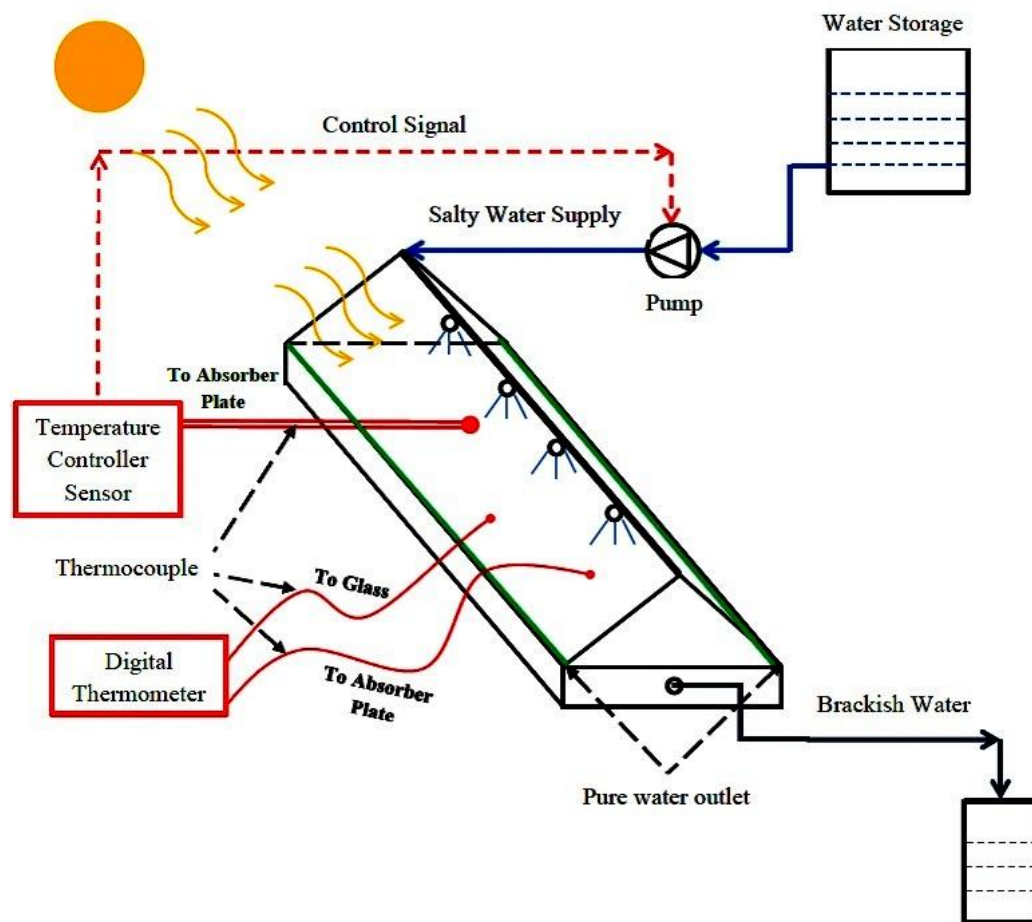


Figure 3.8. System operating diagram

### **3.4.2 Thermocouples**

The k-type thermocouples are used for temperature measurements. The temperatures that are important for the performance are the ambient temperature, absorber plate temperature, feedwater and outlet temperature of brackish water, air temperature in the DS-ISWD and glass temperature. The k-type thermocouples were placed in several points within the system to obtain the necessary temperatures.

With a  $\pm 0.5^{\circ}\text{C}$  accuracy, the data taken for the temperature using the k-type thermocouple was retrieved with two-channel digital thermometer (DM6802A series digital, VICHY). A calibration test was done on the thermocouple and the result was in line the given accuracy from the producer ( $\pm 0.25$ ). Figure 3.9 shows the two-channel digital thermometer.

### **3.4.3 An Eppley Pyranometer**

The solar radiation on the DS-ISWD was measured using the Eppley Radiometer Pyranometer with Omega 0.25% basic DC and with  $\pm 0.5$  accuracy, hourly solar radiation measurements were taken. Figure 3.10 shows an Eppley Pyranometer



Figure 3.9. Two-channel digital thermometer (DM6802A series digital, VICHY)



Figure 3.10. An Eppley Pyranometer

### 3.4.4 Temperature Controller

This equipment used for controlling the temperature, is also called a heat sensor. Temperature controller has the ability to set in different temperature between intervals of -50 to +150 °C. The temperature controller that is used for the solar desalination system is nux hanyoung, model:BR6, this temperature controller with display accuracy  $\pm 1\%$  of FS  $\pm 1$  digit will switch the system on or off at the specified temperature by setting the sensor on the absorber plate. The controller turns on and off the electric water pump according to the set temperatures. Figure 3.11 shows the temperature controller.



Figure 3.11. Temperature controller (nux hanyoung, model:BR6)



## Chapter 4

### RESULTS AND DISCUSSION

This chapter presents the performance of a DS-ISWD at different absorber plate temperatures. The experiments were conducted under the clear sky climatic conditions in the city of Famagusta, North Cyprus with 35° latitude and 33° longitude. The experimental data was recorded in two different weather conditions during spring and summer months on clear sky days. The data were taken hourly between 7 AM and 5 PM. The sections 4.1 and 4.2 presents the performance of the DS-ISWD based on spring and summer tests.

#### 4.1 Spring Results

The April's data collections were under mild weather condition with the maximum and minimum nominal solar radiation of 850 and 200 W/m<sup>2</sup>. The ambient temperature was substantially lower in the early morning than later on in the day with 5 - 15 °C difference. Figure 4.1 to Figure 4.15 indicate hourly solar radiation, pure water production, and covering glass temperature for various set point temperatures.

The results indicate that both the distilled water yields and solar radiation are highest at the peak hour (between 1PM - 2PM). The highest recorded water production during peaking hour ranged between 5 – 6 E<sup>-4</sup> m<sup>3</sup>. Slight changes in water production were observed before and after peaking hours with nominal range of 3 – 4 E<sup>-4</sup> m<sup>3</sup>.

Figure 4.16 shows the daily average water yield for different absorber plate temperature. The maximum yield was obtained when the temperature of the absorber plate was 55 °C. There was a sharp decrease in the yield when the absorber plate temperature is further increased above 55 °C, so in April, the optimum absorber plate temperature was found to be 55 °C. From Figure 4.1 to Figure 4.15, it is clear that the maximum yield almost occurs at the maximum radiation. During tests in April it was observed that when the absorber temperature was set to 40 °C the spraying process was continuous. When the absorber temperatures are set to 45-60 °C the spraying was intermittent. Therefore, it can be concluded that continues spraying of water does not produce the optimum yield.

The ambient and inner glass temperatures are shown in Fig. 4.3, Fig. 4.6, Fig. 4.9, Fig. 4.12 and Fig. 4.15. As expected both the inner glass temperature and ambient temperature increases as radiation increases and as the radiation decreases both the inner glass temperature and ambient temperature decreases.

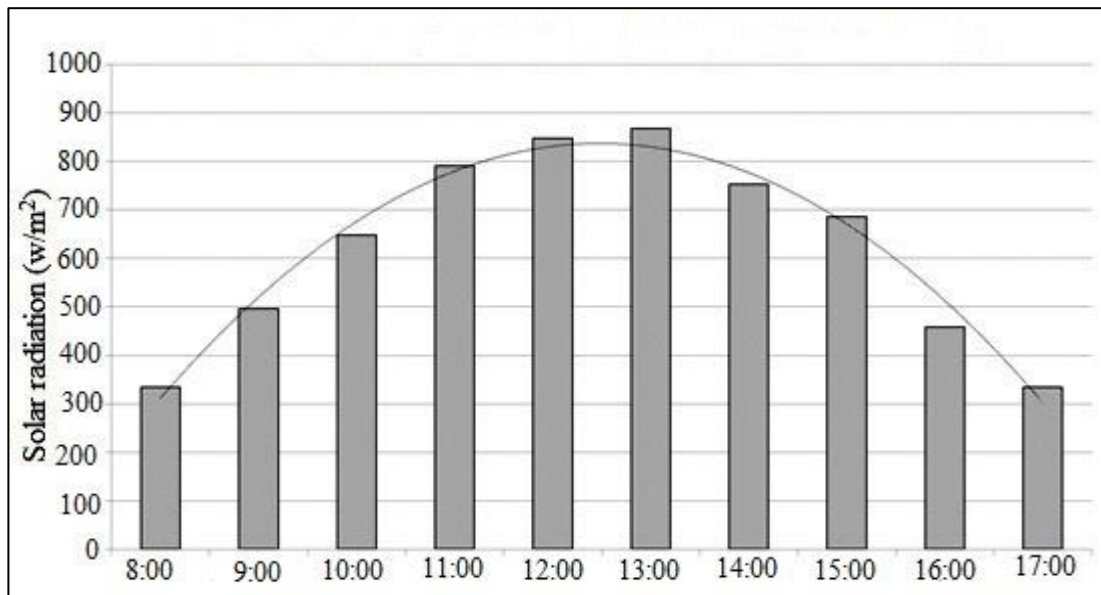


Figure 4.1. Solar radiation at 40 °C set temperature

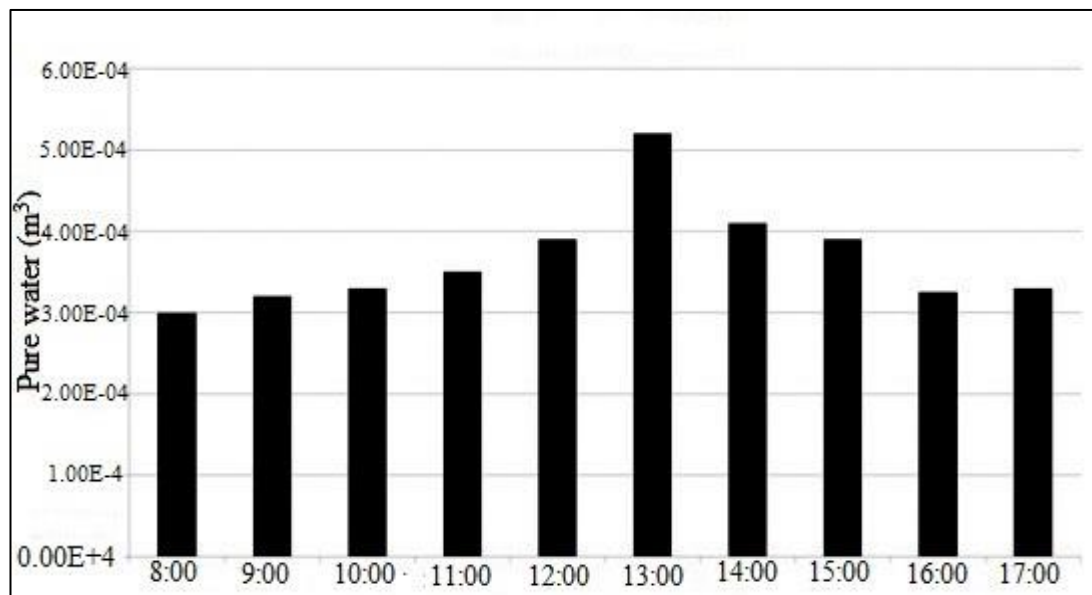


Figure 4.2. Pure water outcome at 40 °C set temperature

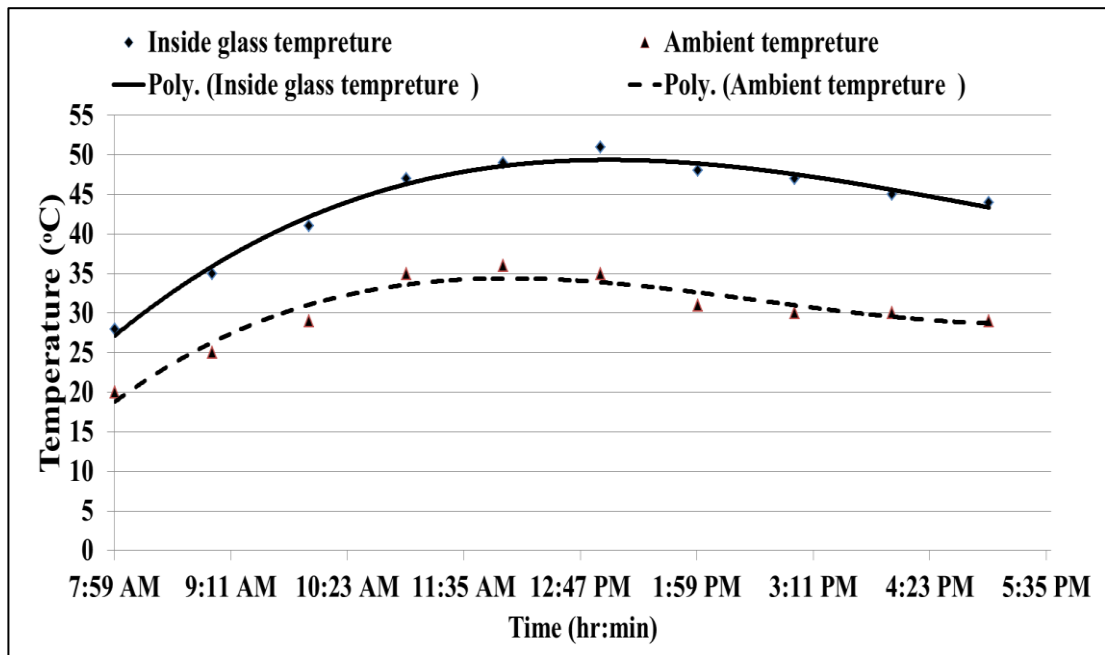


Figure 4.3. Glass temperature and ambient air temperature at 40 °C set temperature

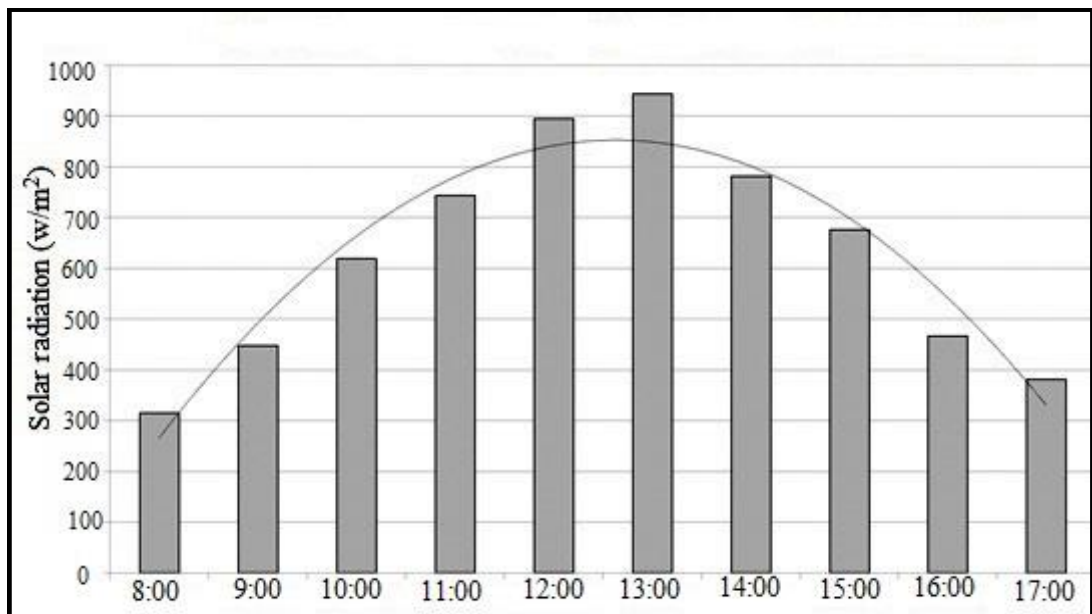


Figure 4.4. Solar radiation at 45 °C set point

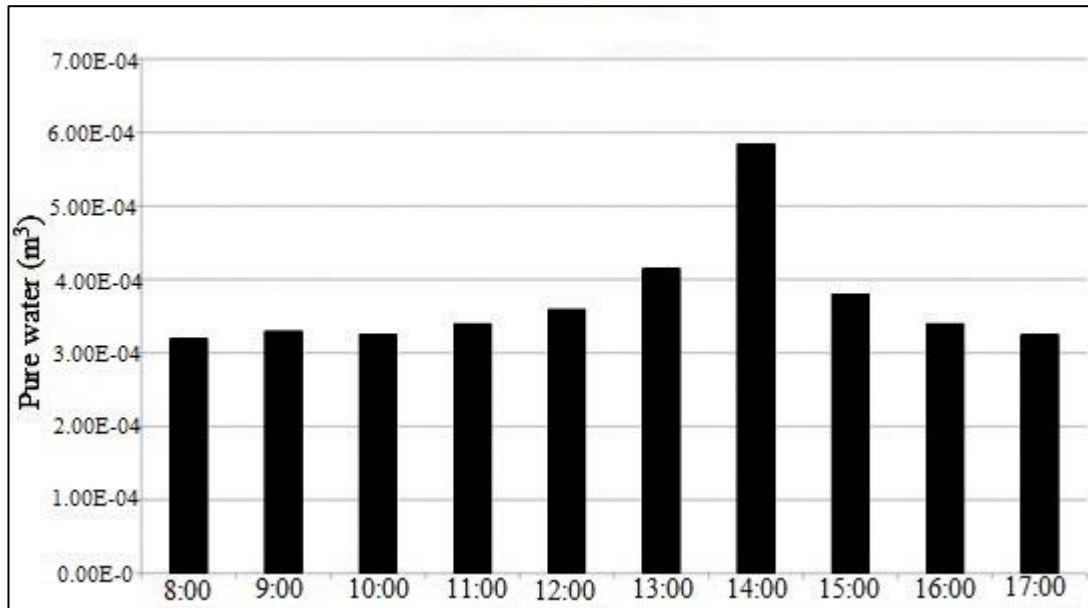


Figure 4.5. Pure water outcome at 45 °C set temperature

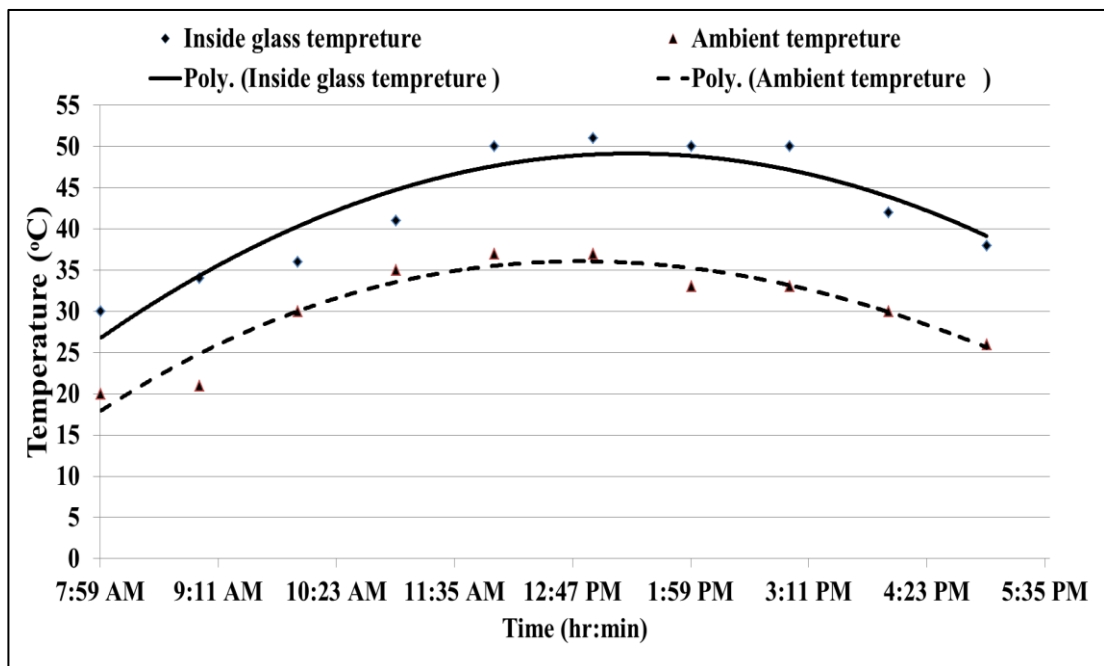


Figure 4.6. Glass temperature and ambient air temperature at 45 °C set point

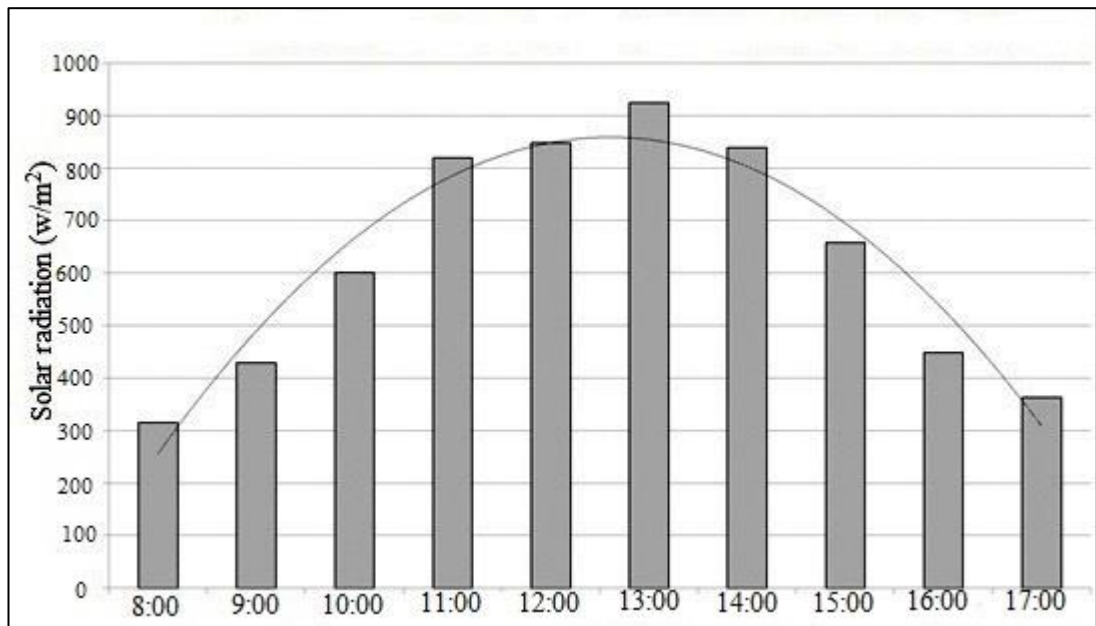


Figure 4.7. Solar radiation at 50 °C set temperature

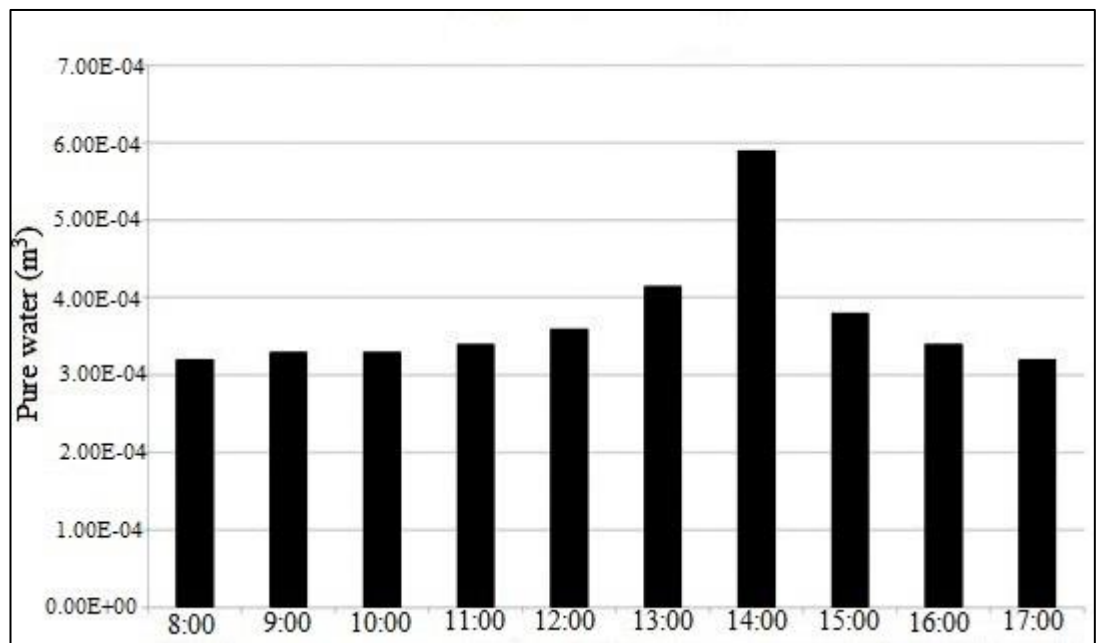


Figure 4.8. Pure water outcome at 50 °C set temperature

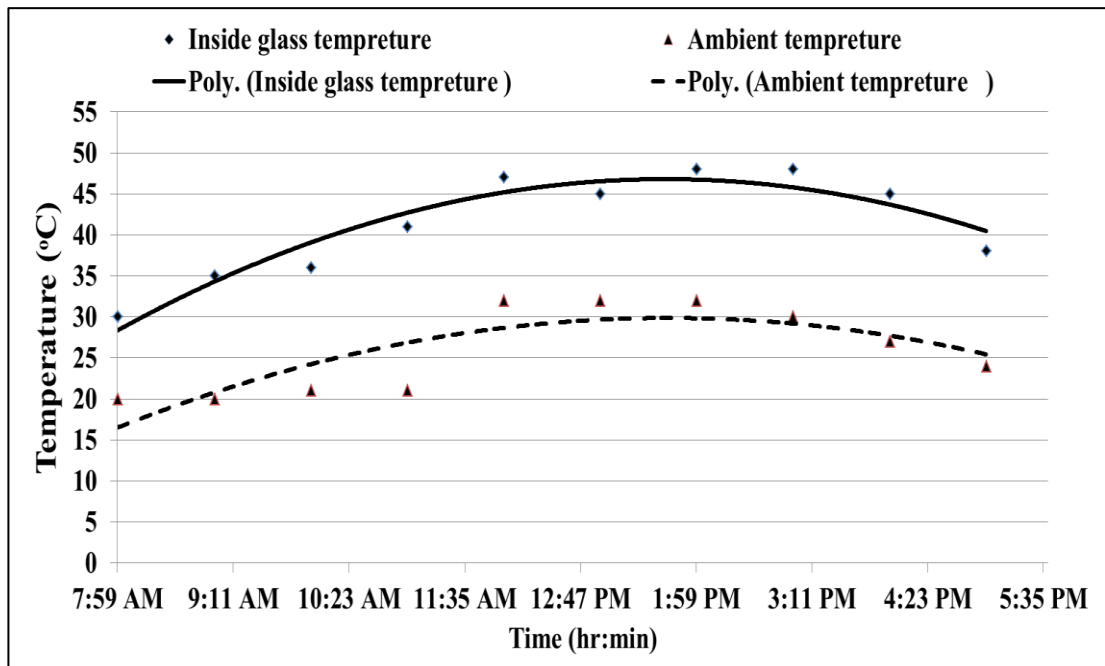


Figure 4.9. Glass temperature and ambient air temperature at 50 °C set temperature

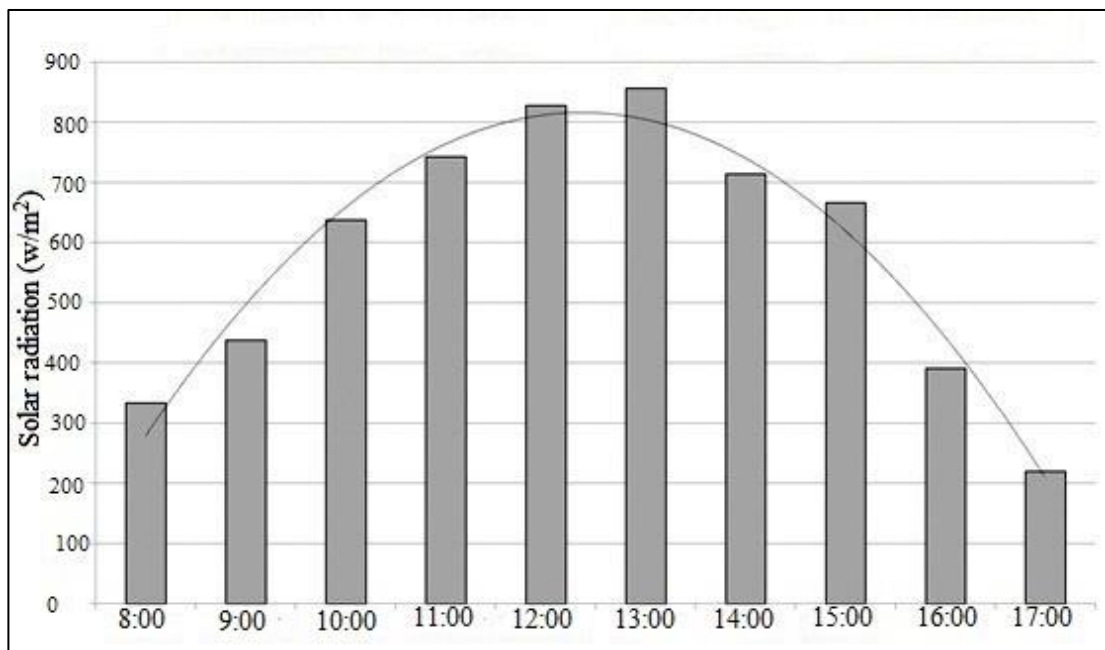


Figure 4.10. Solar radiation at 55 °C set temperature

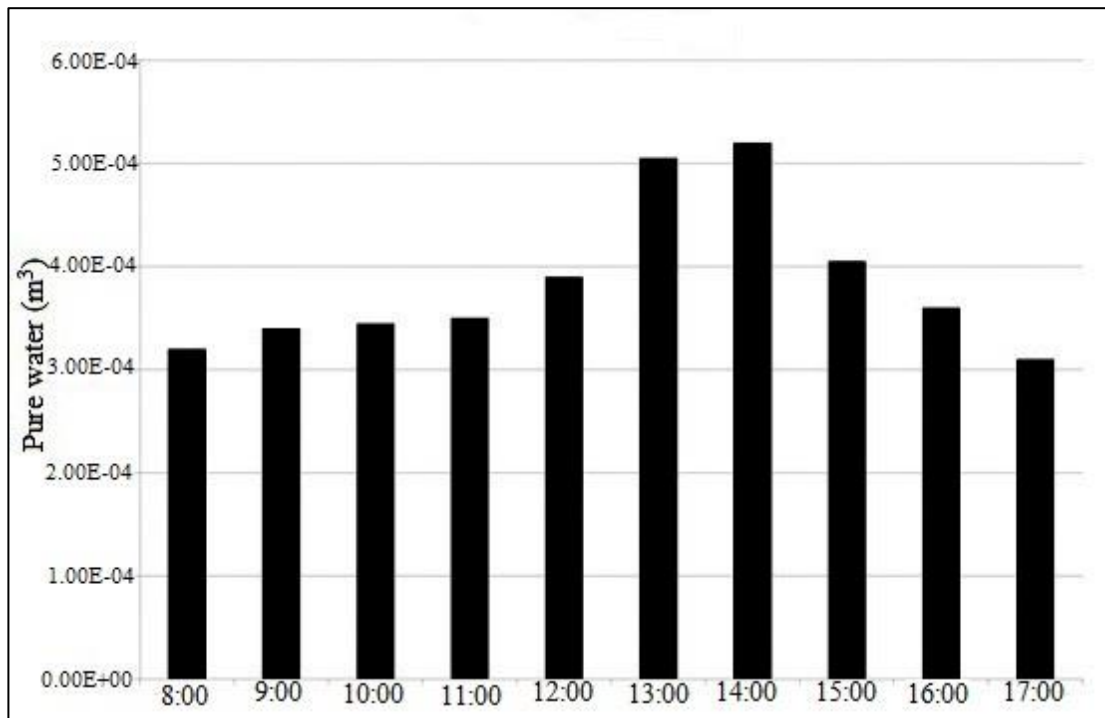


Figure 4.11. Pure water outcome at 55 °C set temperature

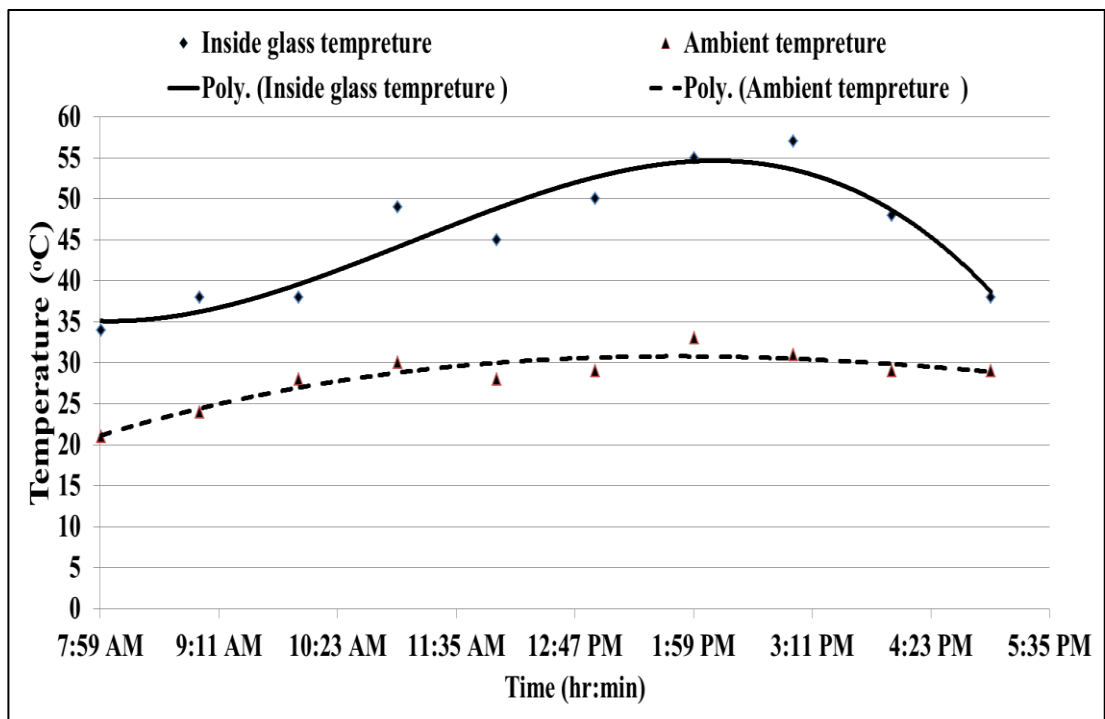


Figure 4.12. Glass temperature and ambient air temperature at 55 °C set temperature



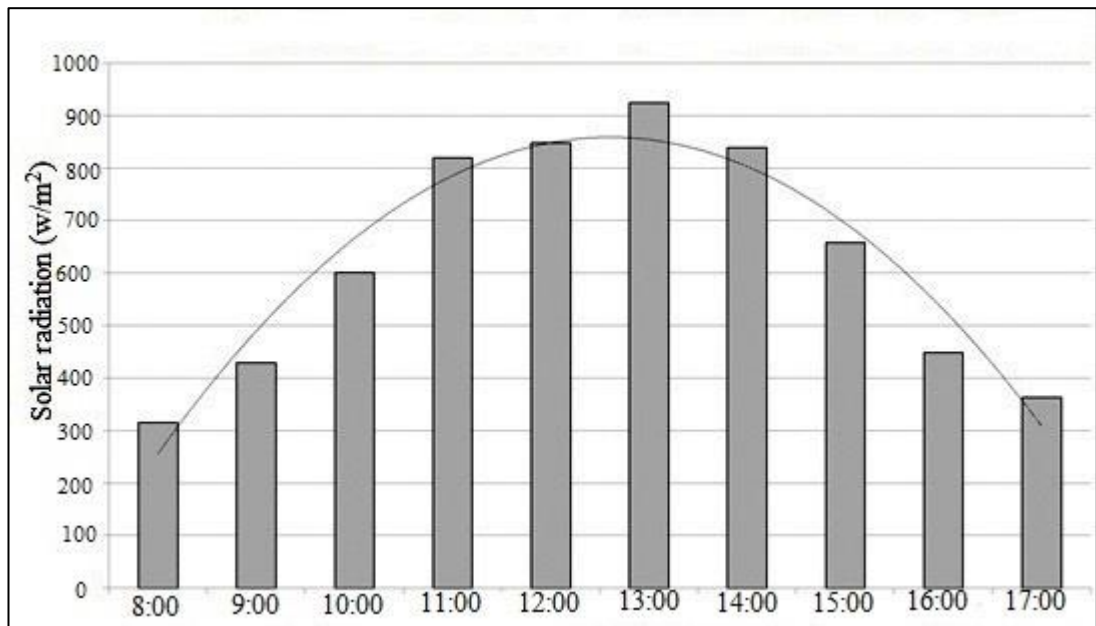


Figure 4.13. Solar radiation at 60 °C set temperature

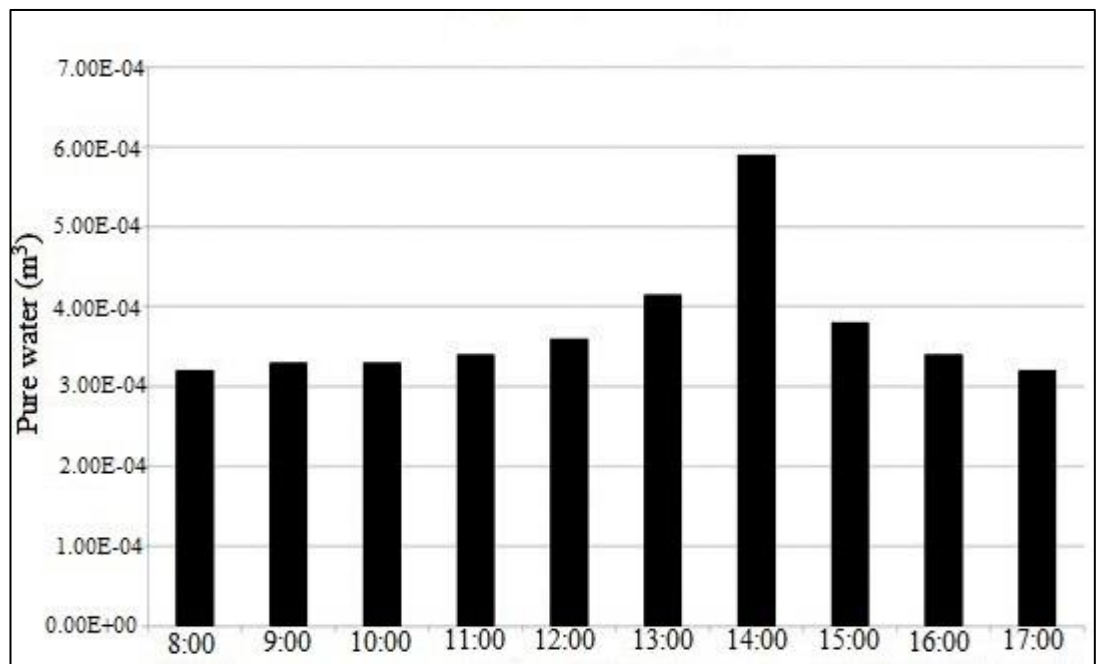


Figure 4.14. Pure water outcome at 60 °C set temperature

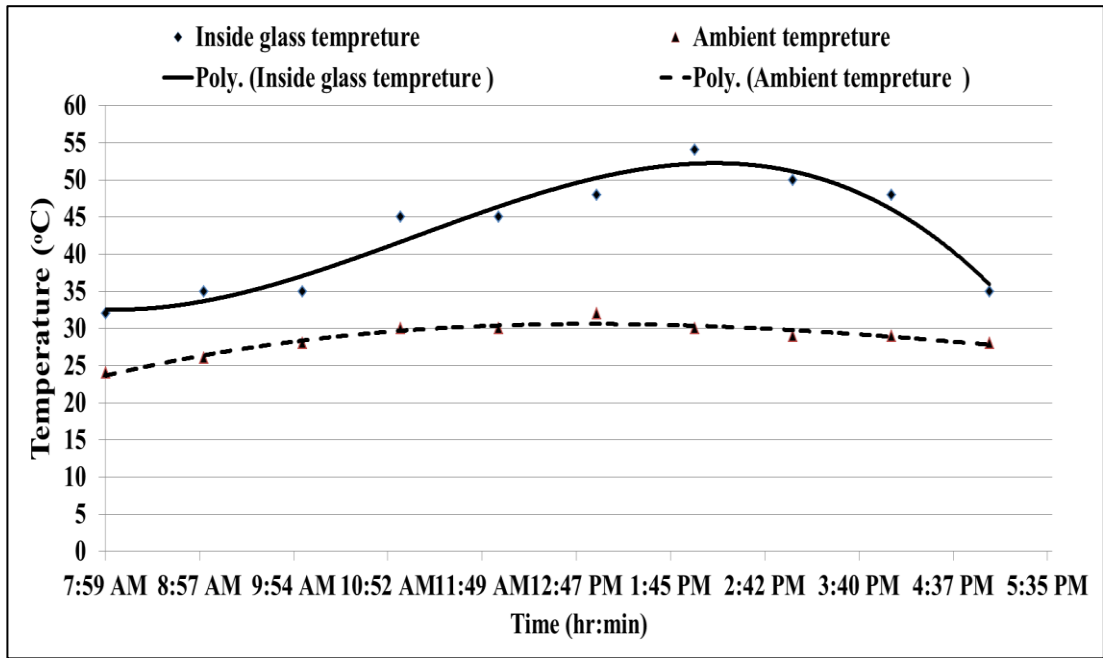


Figure 4.15. Glass temperature and ambient air temperature at 60 °C set temperature

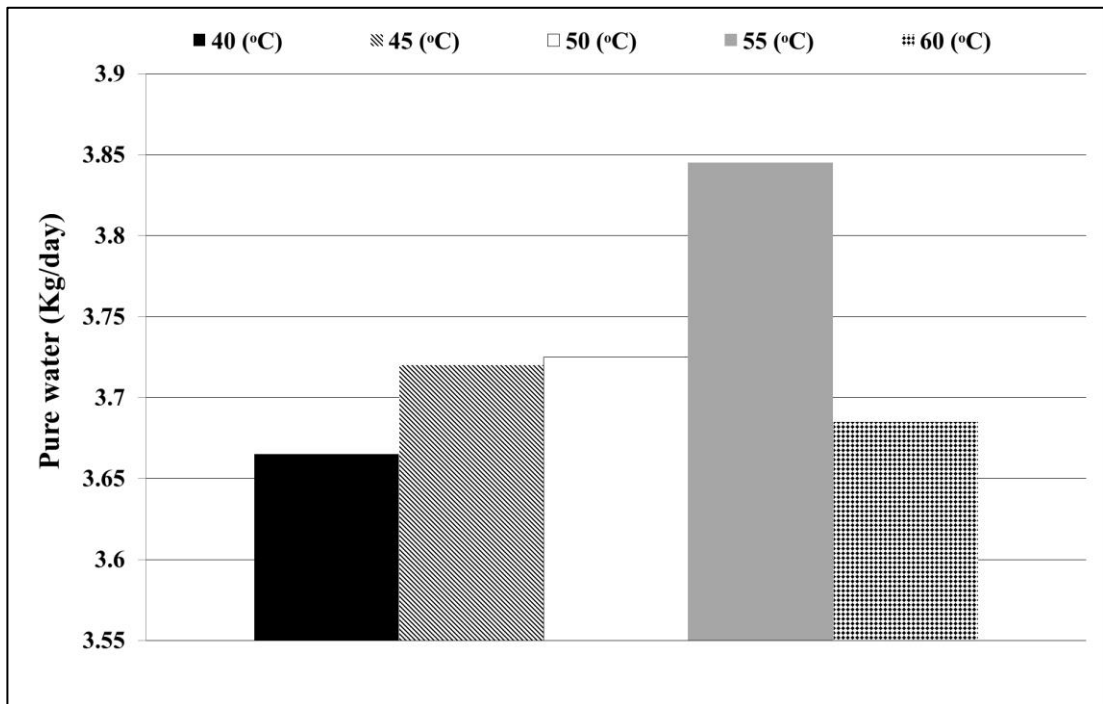


Figure 4.16. Daily average pure water at various set temperatures in spring

The proportion of the energy used for producing water to the rate of total solar radiation is defined as the instantaneous efficiency ( $\eta_i$ ) and can be defined as following,

$$\eta_i = \frac{Q_{ev}}{I_T \times A_b} \quad (4.1)$$

$$Q_{ev} \times M_{ev} \times H \times 3600 = 1 \quad (4.2)$$

$$\eta_{day} = \frac{\int_0^t M_{ev} H dt}{3600 A_b \int_0^t I_T dt} \quad (4.3)$$

Where, H is the latent heat of vaporization (J/kg),  $I_T$  is the total solar radiation falling upon the DS-ISWD surface ( $W/m^2$ ),  $A_b$  is the still base area ( $m^2$ ),  $M_{ev}$  is distilled water production rate ( $kg/m^2h$ ) and  $Q_{ev}$  is the evaporative heat transfer (W). The daily efficiency  $\eta_{day}$  is obtained by adding up the hourly condensate production, multiplying it by the latent heat of vaporization and dividing by the daily average solar radiation over the solar cavity area. The efficiency  $\eta_{day}$  is determined by applying the Eq. 4.3.

The daily efficiency of the DS-ISWD including the pump work input ( $P_{work}$ ) can be found by modifying Eq.(4.3) as follows:

$$\eta_{P,Day} = \frac{\int_0^t M_{ev} H dt}{3600 A_b \int_0^t I_T dt + P_{work}} \quad (4.4)$$

As the feedwater was not continuously supplied to the system it is not appropriate to evaluate the instantaneous efficiency when pump work is taken into consideration. Figure 4.17 indicates the hourly efficiencies of DS-ISWD for different absorber plate temperatures. The hourly efficiencies varied between 19% and 73%. Figure 4.18 shows the daily average efficiency at various set temperatures in spring. The daily average efficiency including the pump work is presented in Fig. 4.19. There is a slight decrease in the system efficiency (i.e., about 6%) when pump work input was considered in the calculations.

The recorded data indicates the efficiencies are higher at 2PM and 5PM. The efficiencies at 2PM are higher for 45 and 50 degrees due to higher solar gain and air-water mixture inside the cavity. Increasing temperature inside the cavity resulted in higher heat loss rate through the glass cover this can be seen in Figure 4.6 and Figure 4.9. The high efficiencies at 5PM are found for 55 and 60 degrees due to stored latent heat inside the solar desalination system. The higher set temperature resulted in shifting peak hour efficiency from 2:00 PM to 5:00 PM and reaching the highest efficiency at 73%.

The low range of set temperature means more frequently water was sprayed on to the absorber plate. This issue resulted in reducing the air temperature inside the cavity and more brackish water is drained from the DS-ISWD (more energy transfer to the drained brackish water) consequently reduced productivity as shown in Figure 4.16. At higher absorber plate temperatures heat losses to the surrounding also increases. Therefore, yield will also decrease for higher absorber temperatures as heat losses increase. In all set temperatures the almost same range of efficiency pattern was

found from 8AM to 11AM which is generally resulted from delay in heating the solar collector.

#### **4.2 Parameters Affecting the Performance of the DS-ISWD**

As mentioned earlier, the heat removal mechanisms during spray cooling are very complex (out of scope of this study). The main reason is the dependence of heat transfer on many parameters such as:

- Droplet size distribution,
- Velocity.
- Droplet number density.
- The orientation of the absorber plate
- Surface roughness of the absorber plate .
- The number of spray jets.
- Gas content.
- Impact of angle.

Although, the performance of DS-ISWD affects by spray cooling parameters, however, absorber plate and feeding water temperatures can be considered as two main parameters that can effectively increase evaporation rate. Since, increasing the temperature of these parameters mean more energy was added to the feeding water to change phase from liquid to vapour.

Apart from above mentioned, the rate of vapour-liquid phase change (condensation) is also an important parameter that can drastically increase water production and performance of the system. The main parameter affecting condensation rate is glass cover temperature in which generally depends on ambient air temperature, glass

thermal property (conductivity, thickness, etc) and in case of external cooling, the temperature of the coolant, and it is well established that minimizing water dept is one of the most vital key features to enhance the performance of solar stills.

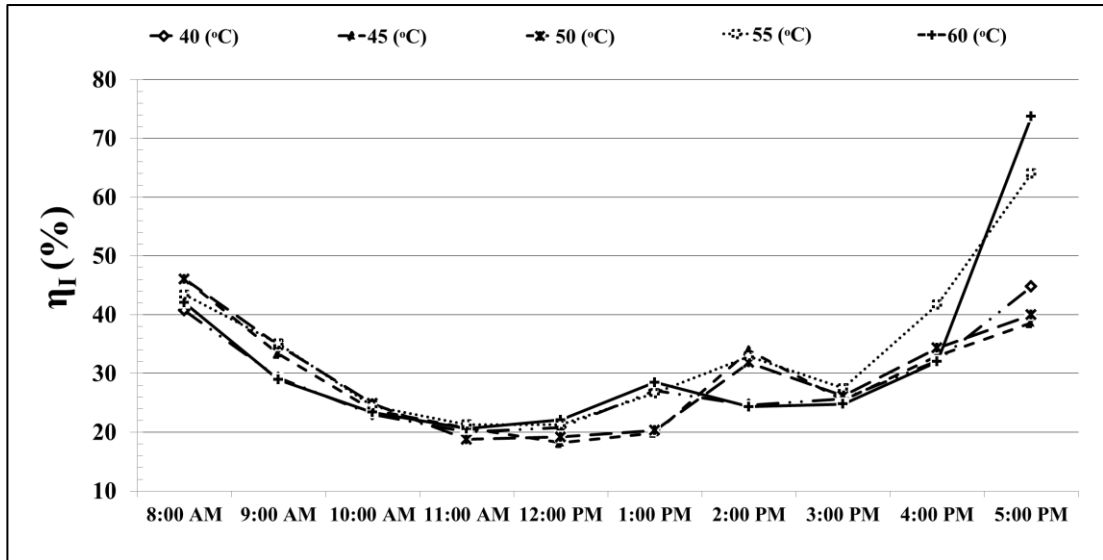


Figure 4.17. Hourly efficiencies of the DS-ISWD in spring at various set temperatures

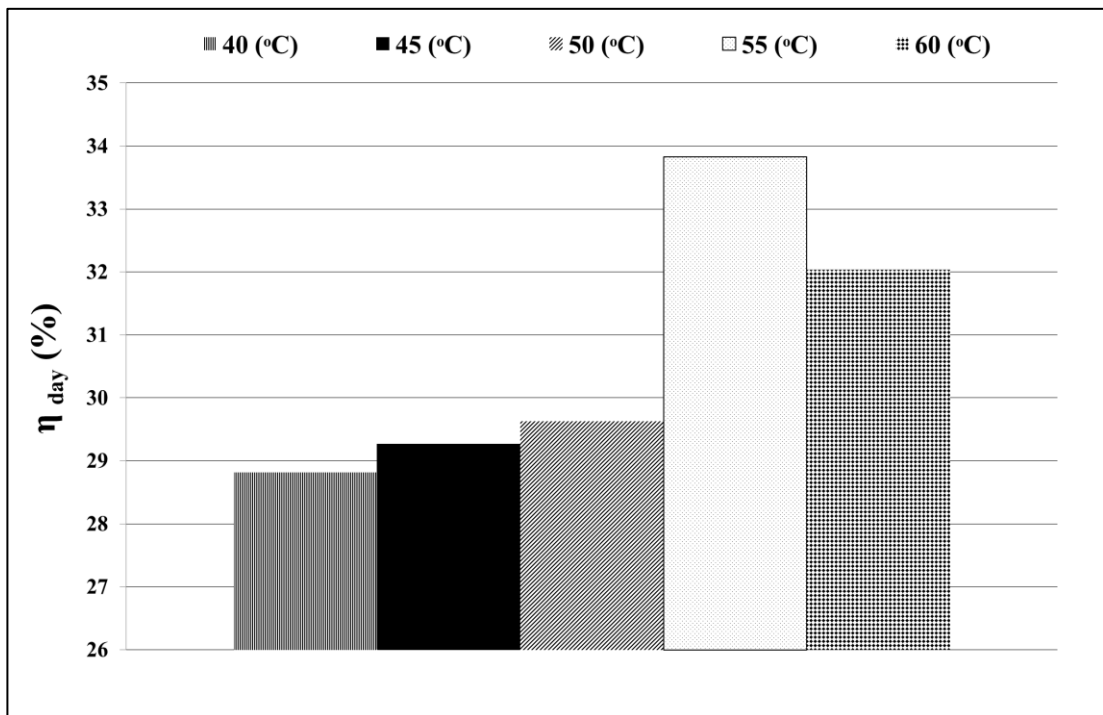


Figure 4.18. Daily average efficiency at various set temperatures in spring

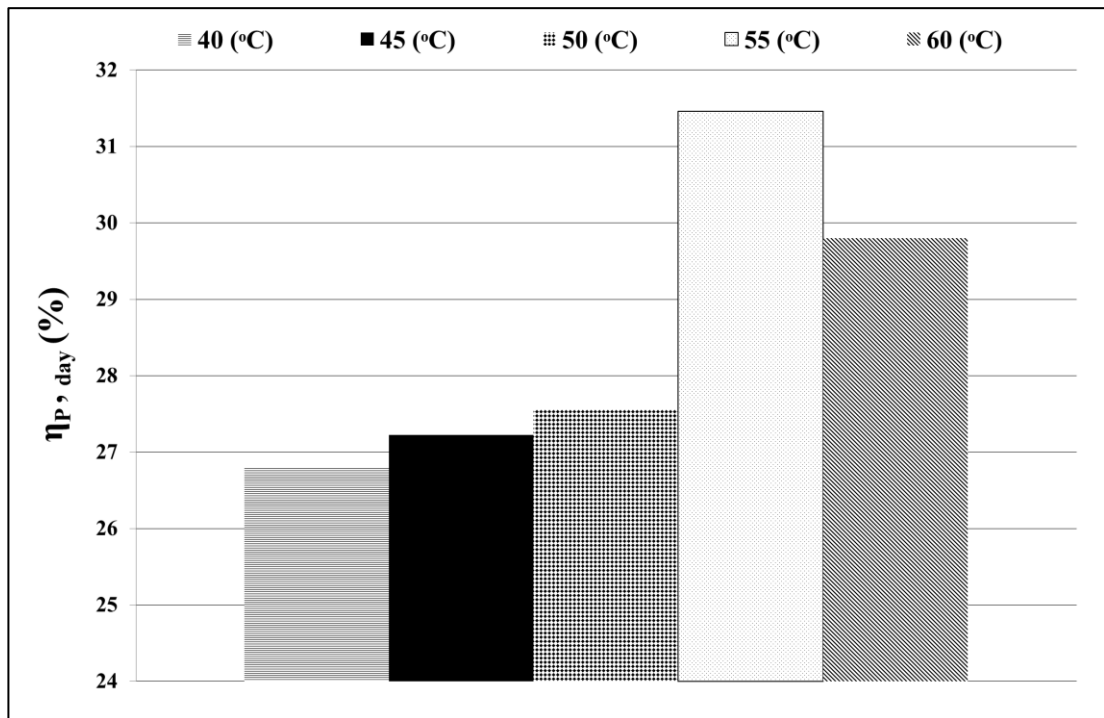


Figure 4.19. Daily average efficiency at various set temperatures in spring including pump work

### 4.3 Summer Results

The summer's data collections were under sunny and warm weather condition and consequently an average ambient temperature was higher than spring. The higher set point temperatures (60 – 70 °C) were examined in July (Figure 4.20 - Figure 4.28). The results indicated the highest rate of water production and solar radiations are during peaking hours were similar to April's data. Although, the highest recorded water production is similar to spring's outcome ( $5 - 6 E^{-4} m^3$ ), higher water production was observed before and after peaking hours with nominal range of  $3.5 - 5 E^{-4} m^3$ .

The hourly rate of change in water production at 60 °C set point temperature indicates the similar pattern as spring with the slight changes before and after peaking hours. While, for 65 and 70 °C, the higher distillation rate was observed

during early operation than afternoon. This is due to higher air temperature inside the cavity during afternoon than before noon. As shown in Figure 4.29, the maximum yield obtained was 4.6 kg/day m<sup>2</sup> when the temperature of the absorber plate was kept at 65 °C which was followed by 4.4 kg/day m<sup>2</sup> for both 60 and 70 °C temperatures.

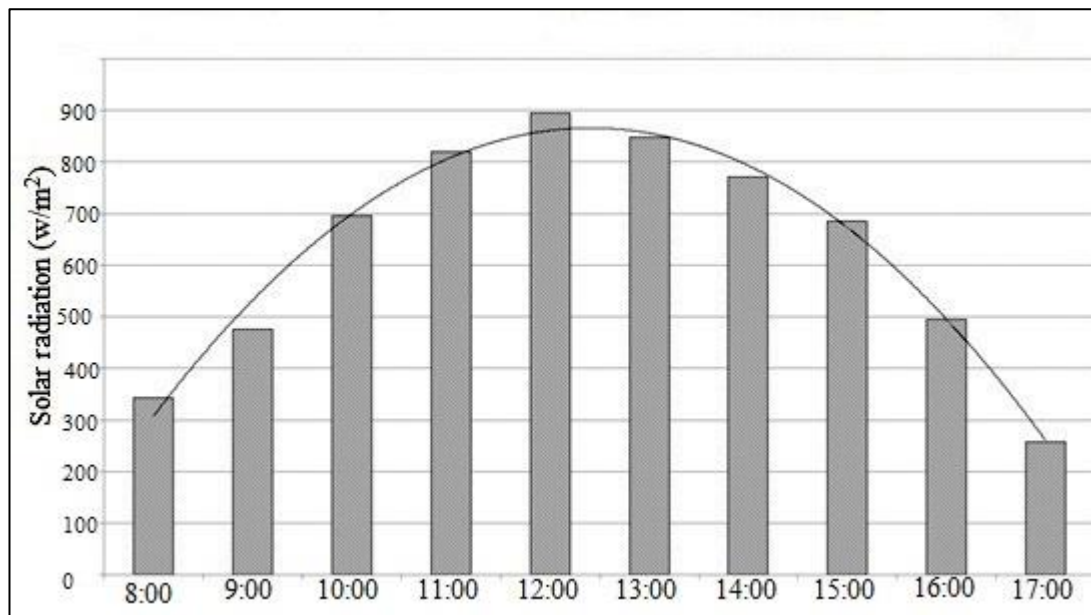


Figure 4.20. Solar radiation at 60 °C set temperature

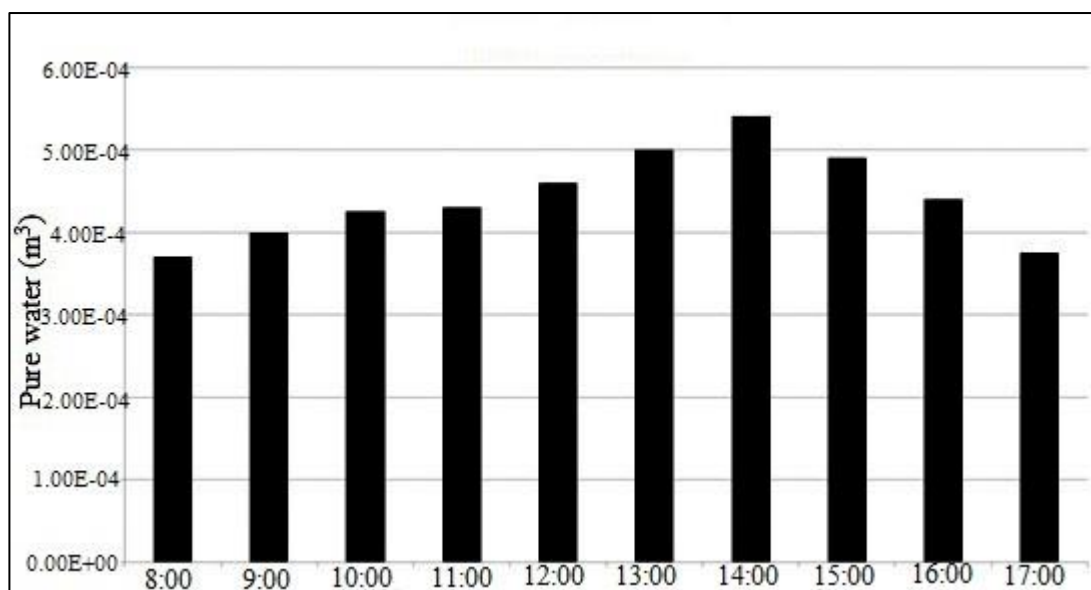


Figure 4.21. Pure water outcome at 60 °C set temperature



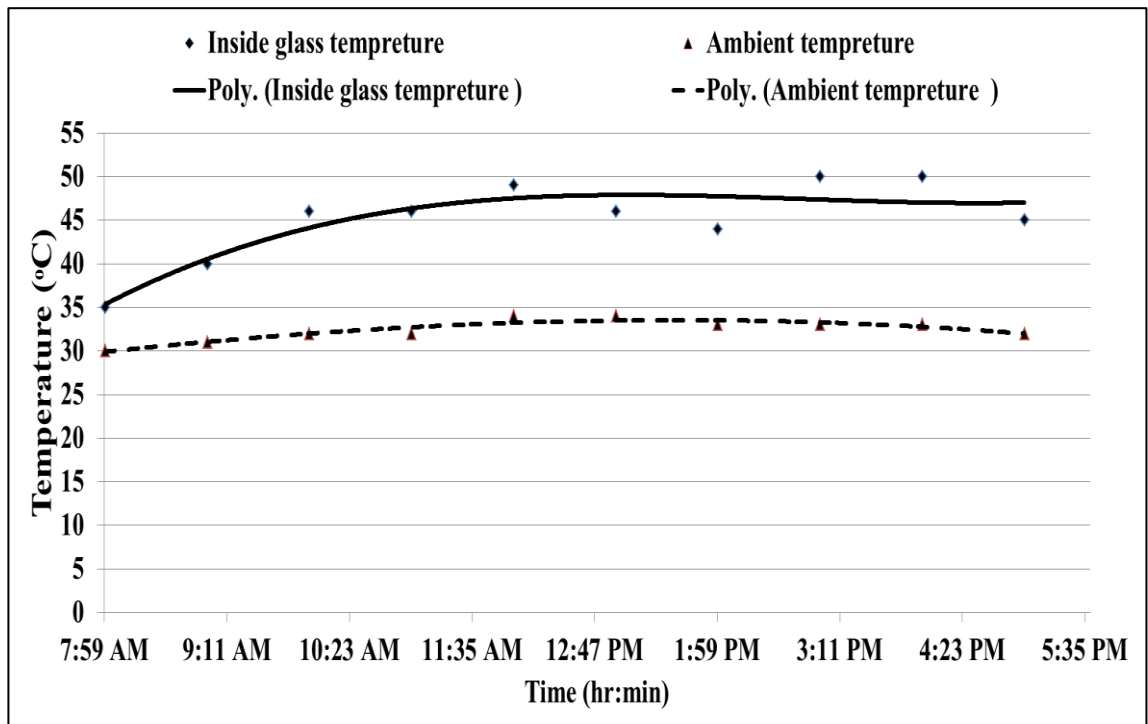


Figure 4.22. Glass temperature and ambient air at 60 °C set temperature

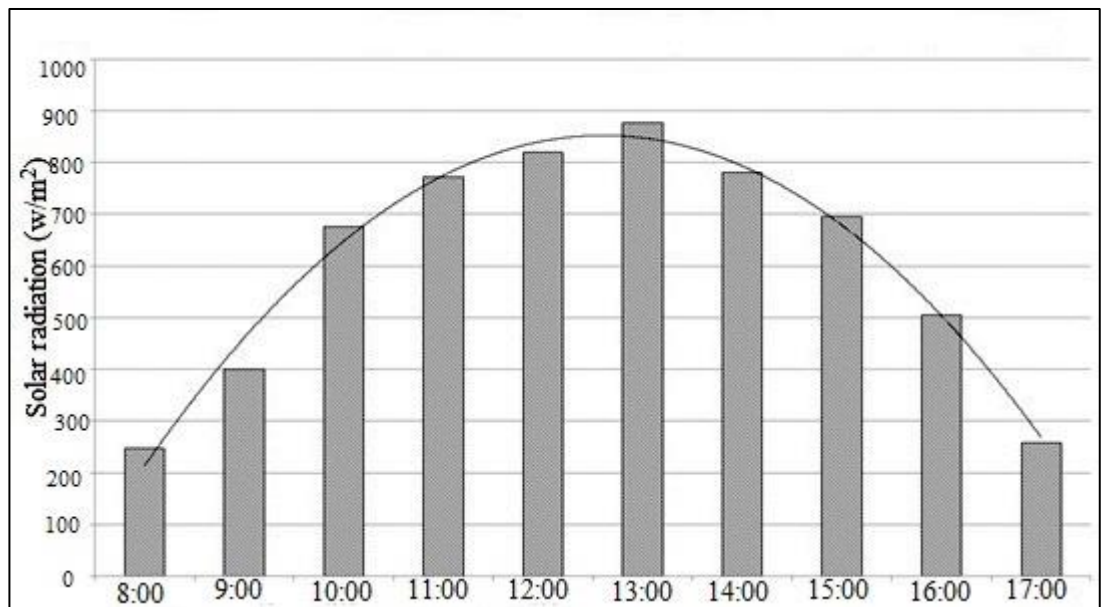


Figure 4.23. Solar radiation at 65 °C set temperature

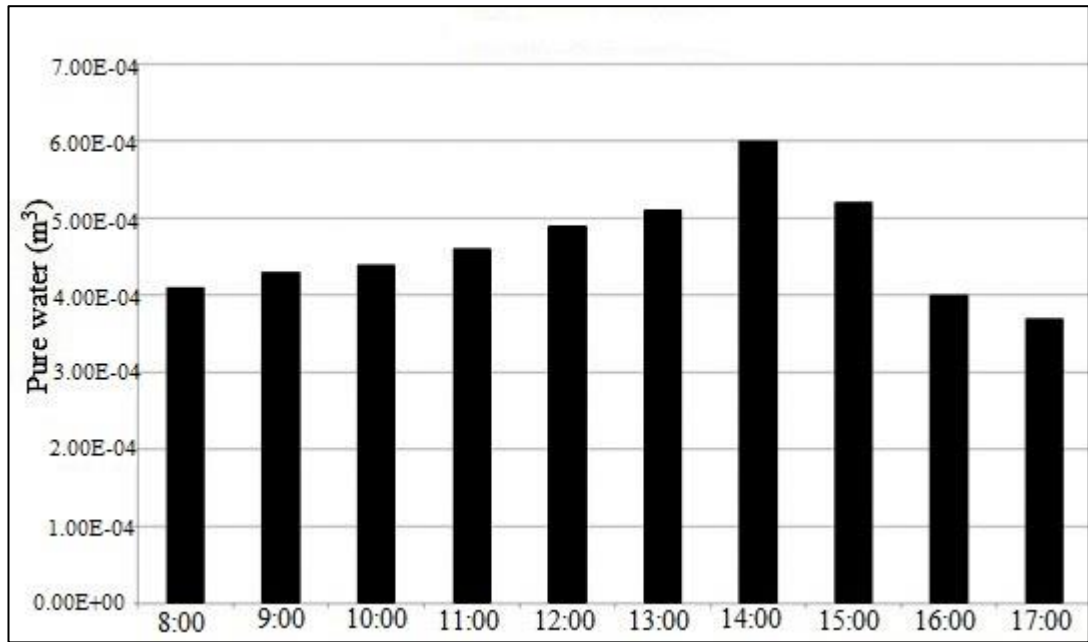


Figure 4.24. Pure water outcome at 65 °C set temperature

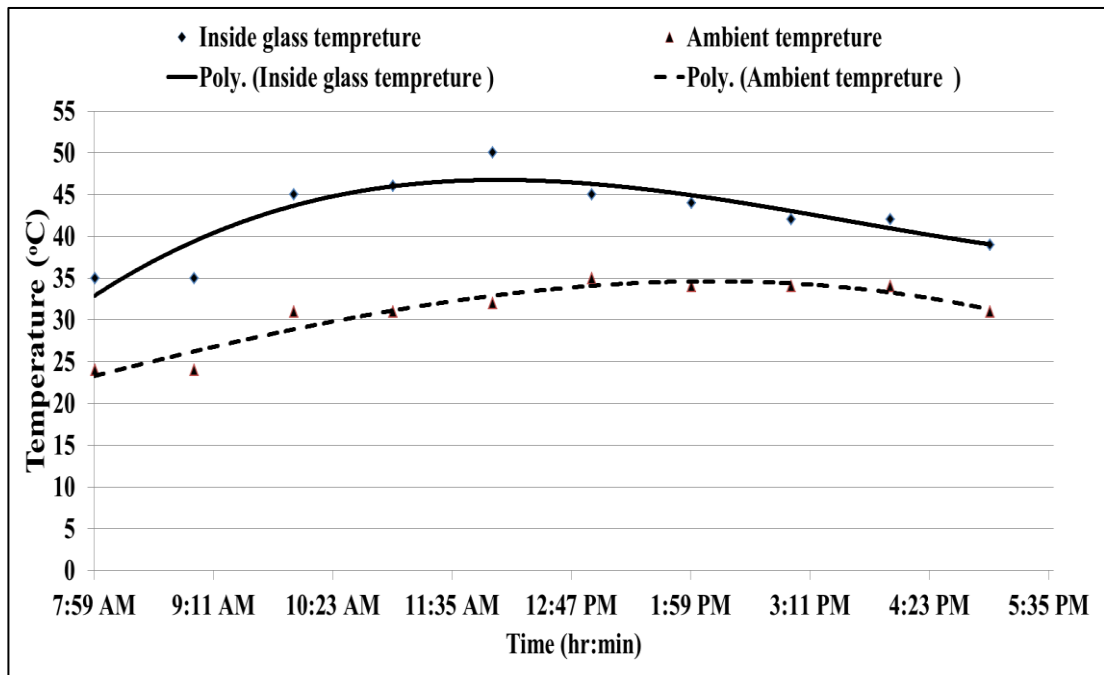


Figure 4.25. Glass temperature and ambient air temperature at 65 °C set temperature

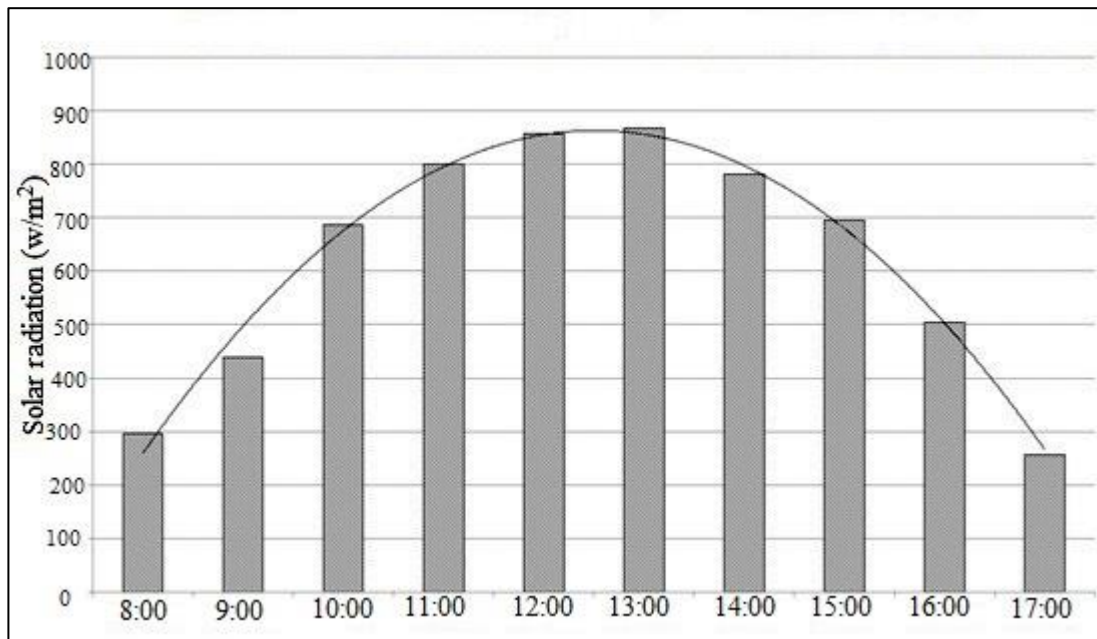


Figure 4.26. Solar radiation at 70 °C set temperature

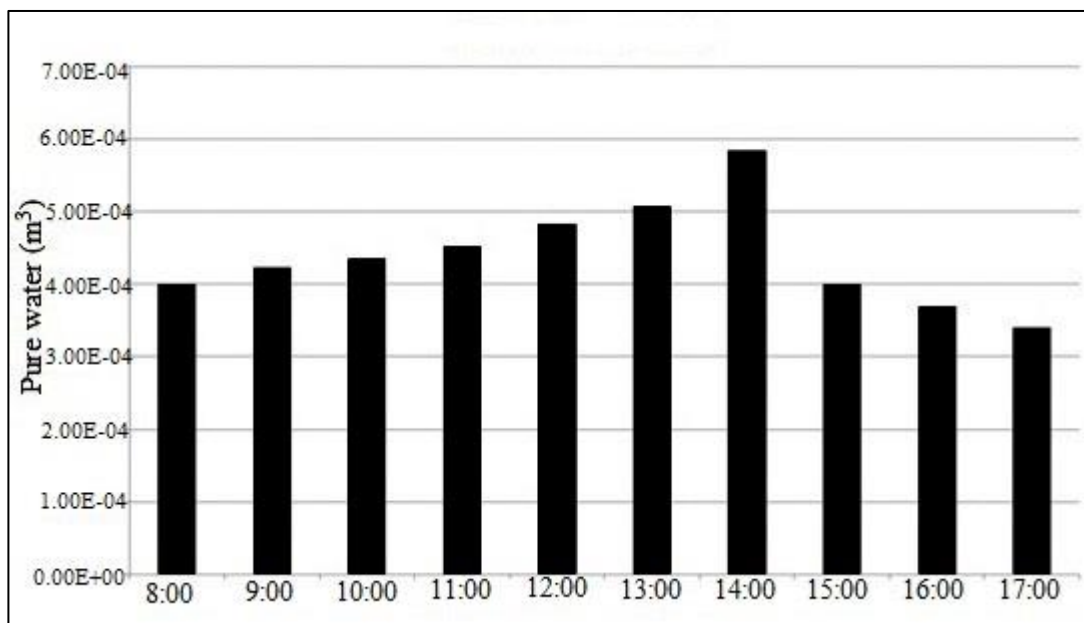


Figure 4.27. Pure water outcome at 70 °C set temperature

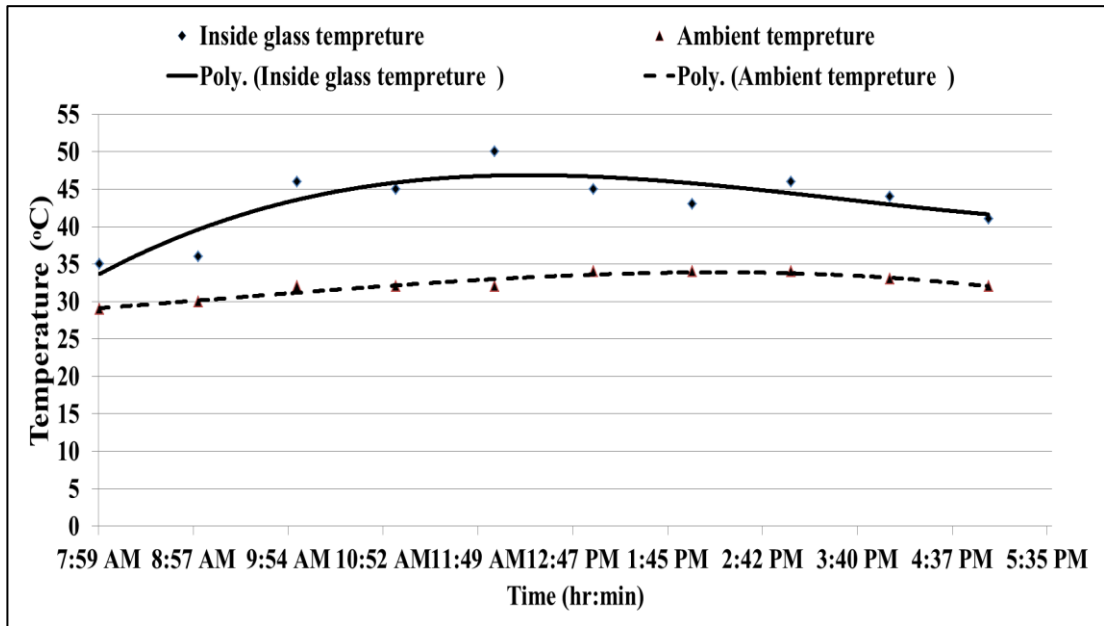


Figure 4.28. Glass temperature and ambient air temperature at 70 °C set temperature

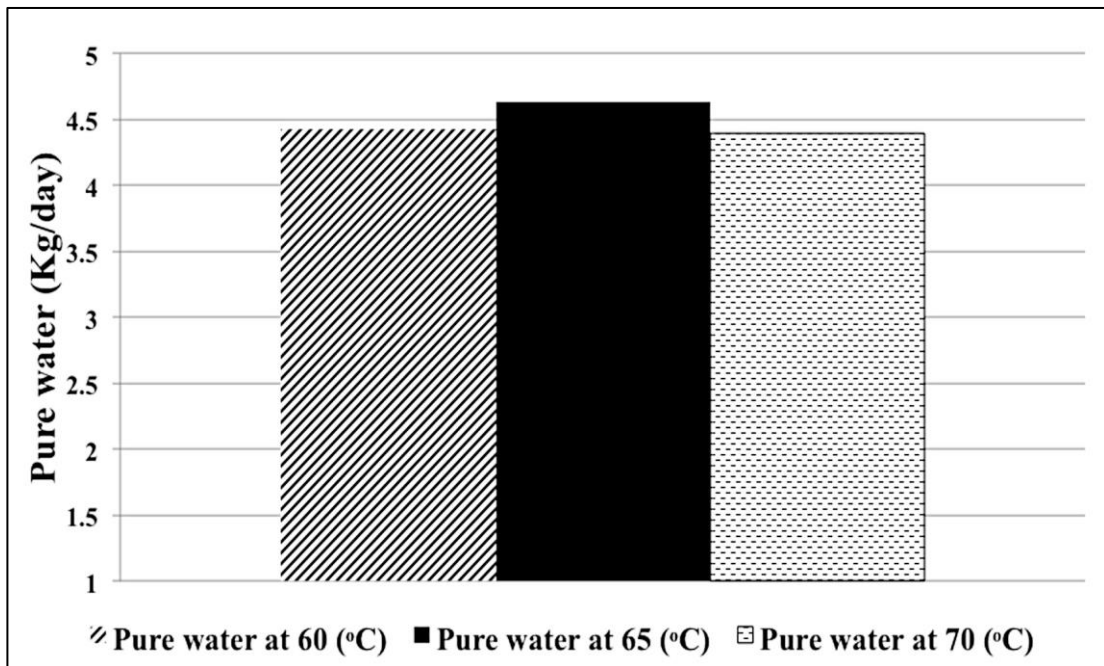


Figure 4.29. Daily average pure water at various set temperature in summer

Figure 4.30 indicates the efficiency comparison among testing days ranging from 22% -32% (at 10AM -3PM) to 75% and 65% (at 8AM and 5PM). As it is mentioned earlier, higher absorber plate temperatures or less frequently water spray results in higher heat losses to the surrounding and thus low productivity. Therefore, this

resulted in low efficiency during mid-operating hours and overall efficiency of the system. The recorded data indicates the efficiencies are higher at 8AM and 5PM for all three set temperatures. The highest and lowest efficiencies at 8PM are found for 65 and 60 °C were 75% and 49% respectively. The higher efficiency during early operation and late afternoon is due to lower solar insolation, lower ambient temperature (condensation improvement), and lower heat loss to the surroundings. This fact was similarly observed during April data collection at the high set point temperatures. The daily average efficiencies excluding pump work at various set temperatures in summer are presented Fig. 4.31. Similarly the daily average efficiencies including the pump work are presented in Fig. 4.32.

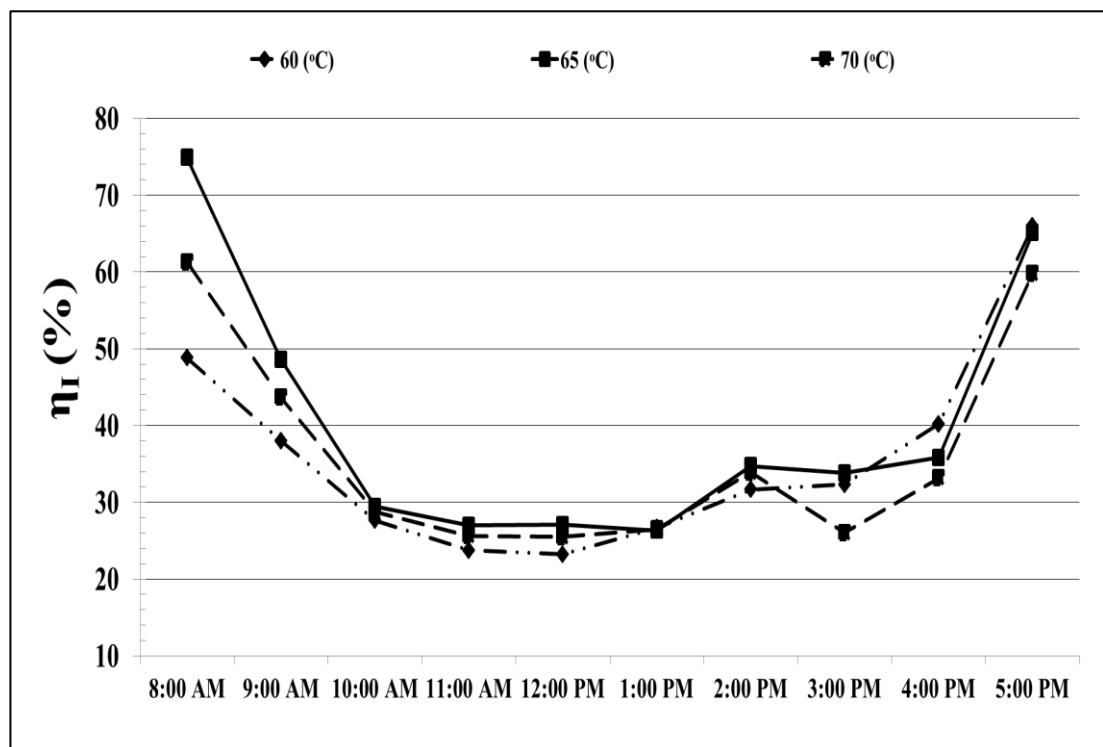


Figure 4.30. Hourly efficiencies of the DS-ISWD in summer

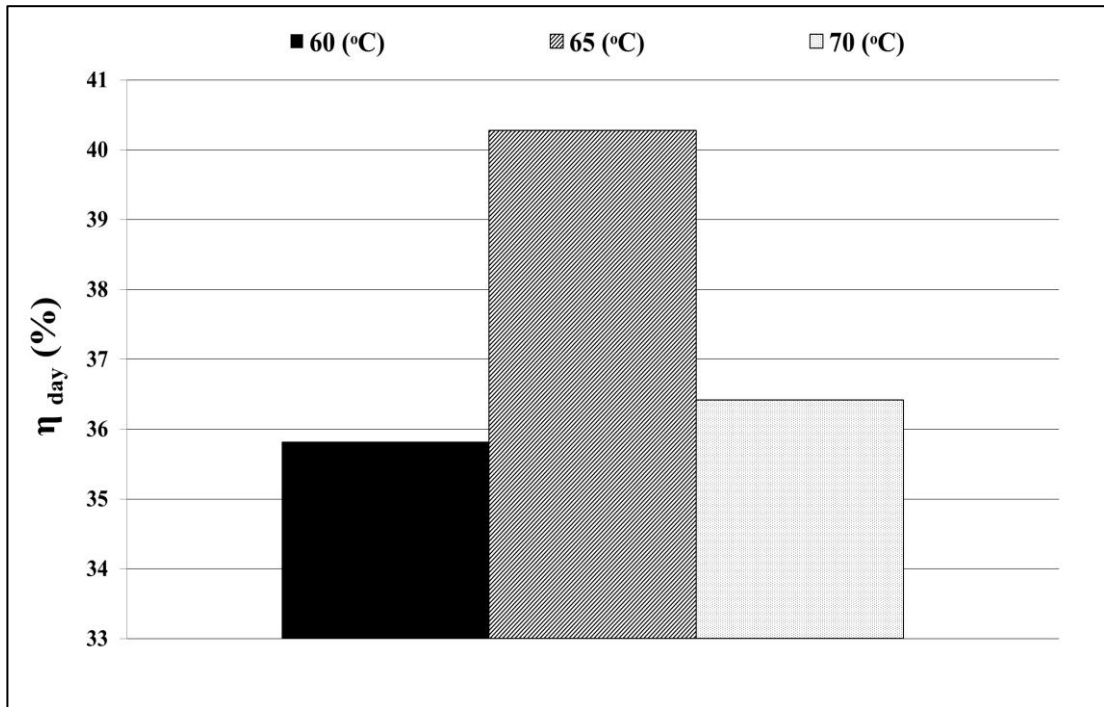


Figure 4.31. Daily average efficiency at various set temperatures in summer

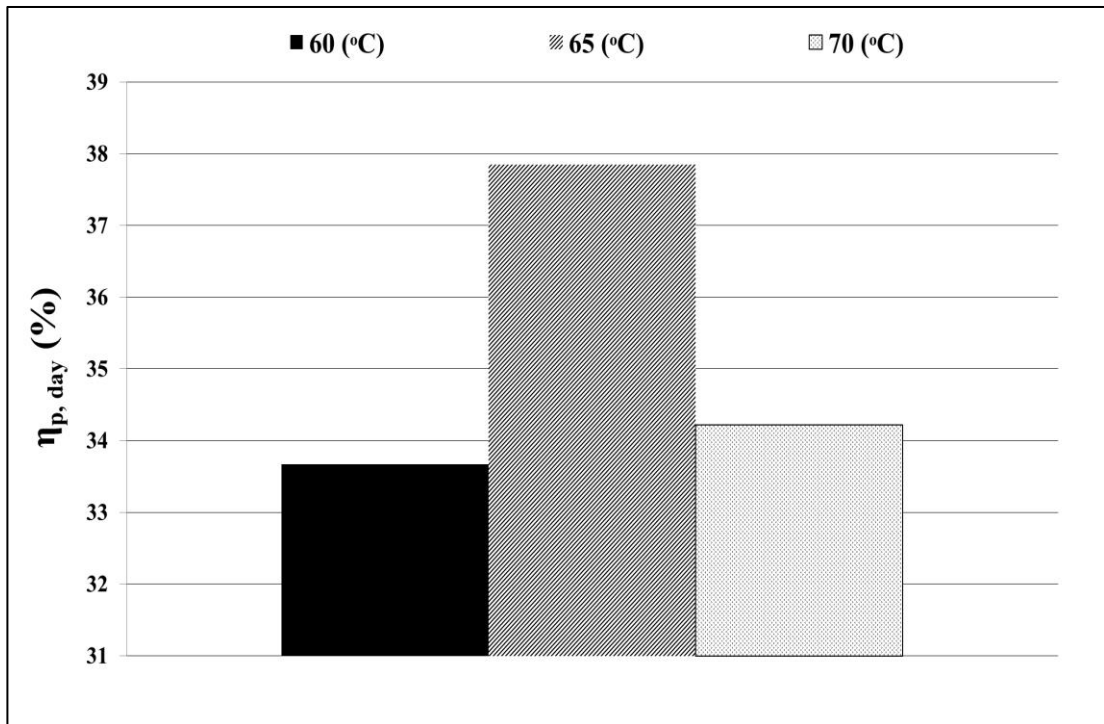


Figure 4.32. Daily average efficiency at various set temperatures in summer including pump work

#### 4.4 Economical Analysis

The cost of producing potable water using DS-ISWD is important in deciding if the system is economically feasible or not. A simple payback period was employed to see if the proposed system is economically feasible. Table 4.1 lists the components prices used in manufacturing the DS-ISWD. The total cost of the system is 756 TL.

Table 4.1. Components price

<b>Component</b>	<b>Price(TL)</b>
Absorber plate	50
Box	150
Temperature controller	150
Pipe	30
Pump	200
Glass	50
Jet spray	52
Fiber glass	50
Matt paint	24
<b><u>TOTAL COST:</u></b>	<b><u>756</u></b>

Various costs encountered in water production and other parameters required for the economic analysis are listed below:

Electricity price: 0.5 TL / kW

Fresh water price: 0.25 TL/Liter

Water productivity: 4.2 Liters/day

Average water productivity: 4 Liters/ day

Pump electricity consumption: 0.33 kWh/day

The cost equation is presented below:

$$Cost = IV + bx \quad (4.5)$$

Where,  $IV$  is the initial investment (i.e., 756 TL),  $b$  is the electricity cost for water production (i.e., 0.04 TL/L) and  $x$  is the water produced in liters.

The cost equation for this system can be written as

$$Cost = 756 + 0.04x \quad (4.6)$$

The saving (S) equation is;

$$S = 0.25x \quad (4.7)$$

Break-even point will be reached as costs and savings equalize. Equating cost and savings gives  $x = 3600$  liters (i.e., break-even will be reached after 900 operating days). So the estimated payback period is 2.5 years. Figure 4.33 shows the cost, savings vs. water produce.

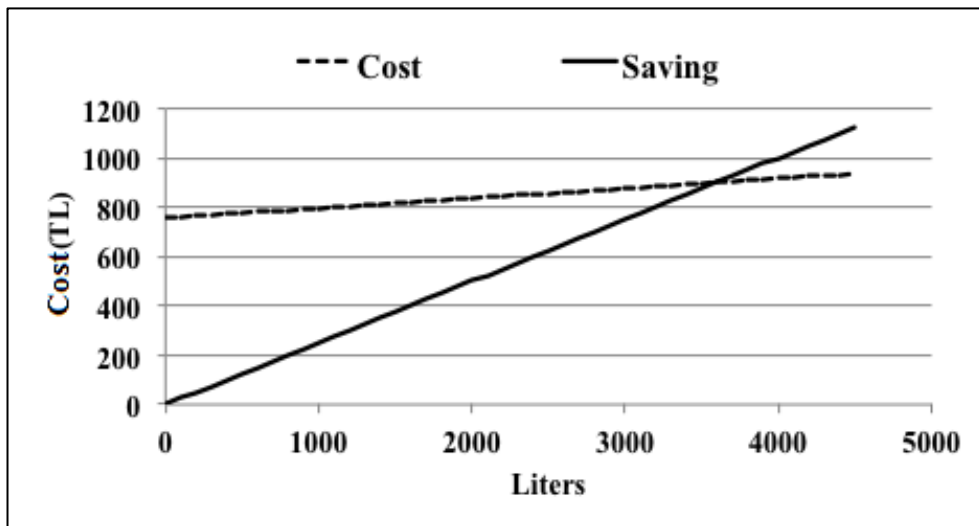


Figure 4.33. Saving and cost Vs. water produced



## Chapter 5

### CONCLUSION AND RECOMMENDATIONS

The DS-ISWD with four jet sprays was tested with different on set temperatures of absorber plate in spring and summer months to find optimum absorber plate temperatures for water production.

The outcomes of spring's data collection indicated that the daily production at 55 °C absorber plate temperature is 19% higher than 40°C, 7.2 % higher than 45 °C, 7 % higher than 50 °C and 9.4 % higher than 60 °C. The daily efficiency of DS-ISWD system was about 33.9% for 55 °C set temperature. In summer weather condition, the daily water production was highest at 65 °C plate temperature. The productivity when 65°C plate temperature used was 5% higher compared to both tests conducted at 60 and 70 °C plate temperatures. The optimum daily efficiency in summer was calculated to be 40% for 65°C set point temperature (i.e., absorber plate temperature). Operating the system continuously does not yield the optimum fresh water production. When the pump work is included in efficiency calculations there is about 6% decrease in the average daily efficiency due pump work input

The main purpose of using a double slope glazing instead of a single slope was the better placement of the feedwater pipe in the system. The pipe can be placed at the middle-top under the glass so adequate distance from the nozzles to the absorber plate can be achieved. If a single sloped ISWD is employed the cavity height should

be increased to allow sprayed water distribution evenly on the absorber plate or put more feedwater pipes and nozzles. The drawback of the DS-ISWD was the difficulty in collecting the condensed water at the lower side of the system. Therefore, it is recommended to use a single slope ISWD rather than a DS-ISWD.

The experimental work has shown that both the amount of feeding water and absorber plate temperatures should be considered together. Reusing feeding water supply is a good method that increases both water production and efficiency of the system and it was studied by many researchers. Therefore, the following could be recommended as future work.

- 1- Using different absorber plates
- 2- Using a single sloped DS-ISWD
- 3- Investigating the effect of inside cavity volume on evaporation rate
- 4- Utilizing different porous media on the plate
- 5- Testing the effect spray jets sizing.

## REFERENCES

- [1] E. T El-Dessouky & H.M Ettouney. Fundamental of salt water desalination. *Elsevier publication*. pp 3.ISBN:0444508104,(2002)
- [2] O.Phillips Agboola & F.Egelioglu, An experimental investigation of an improved incline solar water desalination system in Famagusta. *Scientific Research and Essays* Vol. 6(15), pp. 3298-3308, (11 August, 2011)
- [3] E. Delyannis. Historic Background of desalination and renewable energies. *Solar Energy* 75: 357-366 ,2003
- [4] Qiblawey, H., Banat, F.. Solar thermal desalination technologies, *Desalination*, 220(1-3), 633-644, (2008)
- [5] A.M. El-Zahaby& A.E. Kabeel(October 2010), Enhancement of solar still performance using a reciprocating spray feeding system-An experimental approach, *Desalination*, Vol. 267, pp.209-216.
- [6] H.S. Aybar. Mathematical modeling of an inclined solar water distillation system. *Desalination*, (190: 63-70,2006)
- [7] Garcia-Rodriguez, L., Palmero-Marrero, A., Gomez-Camacho, C., (2002). Comparison of solar thermal technologies for applications in seawater desalination, *Desalination*, 142(2), 135-142.2002

[8] K. Kalidasa Murugavel, P. Anburaj, R. Samuel Hanson, T. Elango, Progresses in inclined type solar stills, *Renewable and Sustainable Energy Reviews*, Volume 20, Pages 364-377, ISSN 1364-0321, (April 2013)

[9] Tanaka T., Yamashita A., Watanabe K., Proc. *International Solar Energy Congress*, Brighton, England 1981;2:1087.

[10] Eduardo Rubio, Miguel A. Porta, José L. Fernández, Cavity geometry influence on mass flow rate for single and double slope solar stills, *Applied Thermal Engineering*, Volume 20, Issue 12, Pages 1105-1111, ISSN 1359-4311, (1 August 2000)

[11] T. Rajaseenivasan, K. Kalidasa Murugavel, Theoretical and experimental investigation on double basin double slope solar still, *Desalination*, Volume 319, , Pages 25-32, ISSN 0011-9164, (14 June 2013)

[12] S. Nijmeh, S. Odeh, B. Akash, Experimental and theoretical study of a single-basin solar still in Jordan, *International Communications in Heat and Mass Transfer*, Volume 32, Issues 3–4, February 2005, Pages 565-572, ISSN 0735-1933,

[13] K. Abdennacer and T. Rachid, Study of the optical performance of a solar still with a double slope and greenhouse effect, *Desalination*, 25000 Constantine, Algeria (2009)

- [14] Edeoja & A. Okibe & Unom, Investigation of the Effect of Angle of Cover Inclination on the Yield Of a Single Basin Solar Still Under Makurdi Climate, Volume 2, Issue 7, Pages 131-138, (2013)
- [15] Pınar İlker Ayav, Gürbüz Atagündüz, Theoretical and experimental investigations on solar distillation of IZTECH campus area seawater, *Desalination*, Volume 208, Issues 1–3, (5 April 2007), Pages 169-180, ISSN 0011-9164
- [16] A.K. Sethi and V.K. Dwivedi, Exergy analysis of double slope active solar still under forced circulation mode, *Desalination*, 51:40-42, 7394-7400 (17 April 2013)
- [17] R. Rajanarthini et al K. Shanmugasundaram, Janarthanan, Performance analysis of double slope wick-type solar still with varying thermal insulation beneath the wick surface 51:10-12, 2076-2086, (22 August 2012)
- [18] S. Shanmugana. B. Janarthanan. J. Chandrasekaran, Performance of single-slope single-basin solar still with sensible heat storage materials , 41:1-3, 195-203, (26 Januar 2012)
- [19] Alaudeen A.a, Syed Abu Thahir A.b, Vasanth K.c, Experimental and theoretical analysis of solar still with glass basin, doi: 10.1080/19443994.2014.888679, (22 January 2014)
- [20] Mahmoud. I.M. Shatat, K. Mahkamov, Determination of rational design parameters of a multi-stage solar water desalination still using transient mathematical modelling, *Renewable Energy*, 35 ,52–61, (4 August 2009)

[21] Rahul Dev, G.N. Tiwari, Annual performance of evacuated tubular collector integrated solar Still, *Desalination*,41:1-3, 204-223, (29 Mar 2012)

[22] Abdulah.S, Solar Desalination System by Humidification Dehumidification Method, *Eastern Mediterranean University*, (January 2013)

[23] Ali. F. Muftah, M.A. Alghoul, Ahmad Fudholi, M.M. Abdul-Majeed, K. Sopian, Factors affecting basin type solar still productivity: A detailed review, *Renewable and Sustainable Energy Reviews*, Volume 32, (April 2014), Pages 430-447, ISSN 1364-0321

[24] J.Kim(November 2006), Spray cooling heat transfer:The state of the art, *Heat And Fluid Flow*, Vol. 28, pp.753-767.

[25] J.L.Xie& R.Zhao(April 2012), Thin liquid film flow and heat transfer under spray impingement, *Applied thermal engineering*, Vol. 48, pp.342-348.